Holocene palaeoenvironmental evolution of the Ebro Delta (Western Mediterranean Sea): Evidence for an early construction based on the benthic foraminiferal record

Alejandro Cearreta[1], Xavier Benito[2, 3], Carles Ibáñez[2], Rosa Trobajo[2] and Liviu Giosan[4]

[1]Departamento de Estratigrafía y Paleontología, Universidad del País Vasco UPV/EHU, Spain (alejandro.cearreta@ehu.eus)

[2]IRTA, Aquatic Ecosystems Program, Catalonia, Spain (xavier.benito@irta.cat, carles.ibanez@irta.cat, rosa.trobajo@irta.cat)

[3]Centre for Climate Change, University Rovira i Virgili, Spain

[4]Woods Hole Oceanographic Institution, USA (lgiosan@whoi.edu)

*Corresponding author. Alejandro Cearreta, Departamento de Estratigrafía y Paleontología, Facultad de Ciencia y Tecnología, Universidad del País Vasco UPV/EHU, Apartado 644, 48080 Bilbao, Spain. Telephone: Tel.: +34 946 012 637, Fax: +34 946 013 500, Email: alejandro.cearreta@ehu.eus

Abstract

Major Mediterranean deltas began to develop during a period between 8000 and 6000 yr BP when the rate of fluvial sediment input overtook the declining rate of sea-level rise. However, different authors have argued that the Ebro Delta primarily formed during the Late Middle Ages as a consequence of increased anthropogenic pressure on its river basin and these arguments are supported by the scarcity of previous geological studies and available radiocarbon dates. To reconstruct the environmental evolution of the Ebro Delta during the Holocene, we used micropalaeontological analysis of continuous boreholes drilled in two different locations (Carlet and Sant Jaume) on the central delta plain. Different lithofacies distributions and associated environments of deposition were defined based on diagnostic foraminiferal assemblages and the application of a palaeowater-depth transfer function. The more landward Carlet sequence shows an older and more proximal progradational delta with a sedimentary record composed of inner bay, lagoonal, and beach materials deposited between 7600 yr BP and >2000 yr BP under rising sea-level and highstand conditions. This phase was followed by a series of delta-plain environments reflected in part by the Carlet deposits that formed before 2000 yr BP. The Sant Jaume borehole is located closer to the present coastline and contains a much younger sequence that accumulated in the last 2.0 ka during the development of three different deltaic lobes under highstand sea-level conditions. The results of the present study reinforce the idea that the Ebro Delta dates to the early Holocene, similar to other large Mediterranean deltas.

Keywords

Ebro Delta, sedimentary sequences, benthic foraminifera, environmental evolution, Mediterranean Sea, Holocene

Introduction

Deltas are the largest coastal landforms in the world (Evans, 2012). These coastal depositional environments result from the interaction between river and marine forces. The strength of both elements determines the dominant processes governing the evolution of deltaic systems through time (Jiménez et al., 1997). The morphology and sedimentary architecture of deltas depend on the relative magnitude of tides, waves and currents (Wright and Coleman, 1973; Galloway, 1975). The morphological evolution of a delta is also controlled by relative sea-level changes, which in turn depend on the eustatic sea-level rise and local subsidence or uplift (Galloway, 1975). Subsidence results naturally from the compaction of deltaic sediments, degassing of peats and growth faults developed at the base of deltaic sediments; however, subsidence can be additionally increased by human activities, such as the extraction of groundwater. Relative sea-level rise (RSLR) can be compensated by vertical accretion processes taking place in the delta plain. The accretion rates depend on fluvial sediment inputs and sea-level rise itself through feedback mechanisms (Day et al., 2011; Ibáñez et al., 2014).

Deltas are considered to be highly vulnerable to even minor changes in relative sea level, particularly because most modern deltas are actively subsiding and their sediment supply has been curtailed (Giosan et al., 2014; IPCC, 2014). Moreover, global warming is accelerating sea-level rise, which intensifies coastal erosion and land loss due to marine inundation (Fatorić and Chelleri, 2012). To implement

science-based coastal protection measures in these sensitive areas, a precise definition of the relationship between sea-level change and delta evolution is critical. Consequently it is essential to understand the relationships between delta development and sea-level changes during the Holocene (Stanley and Warne, 1994). Under natural conditions, deltas have mechanisms to enhance vertical accretion and gain land as a response to RSLR, especially via the increased river avulsion and delta lobe formation in shallow areas and the increased accretion in coastal marshes and beaches connected to marine environments (Ibáñez et al., 2014). This suggests that river-dominated deltas can be resilient to changes in sea level.

Previous analysis of major modern deltas in the Mediterranean Sea showed that these environments started to form between 8000 and 6000 yr BP. Overlying upper Pleistocene fluvial gravels, Holocene deltaic deposits consist of variable aggradational and progradational lithologies (Stanley and Warne, 1994, 1997; Vella et al., 2005; Anthony et al., 2014). These previous works showed that the deceleration in sea-level rise was the key to the initiation of delta formation and that Holocene deltaic sequences began to accumulate as the rate of fluvial sediment input overtook the declining rate of sea-level rise along the coasts. For the northwestern Mediterranean area, Lambeck and Purcell (2005) and Pirazzoli (2005) found a rapid sea-level rise until 6.0 ka, followed by a more gradual increase in sea level with a slight deceleration during the last 1.5 ka, with stabilization for the last 0.5 ka.

Recently, Maselli and Trincardi (2013) supported the idea that the onset of the northern Mediterranean deltas followed an ancestral phase dominated by estuary fill and relatively slow delta growth at approximately 6000 yr BP. Furthermore, they suggested that these deltas formed almost synchronously during two short intervals of

enhanced anthropogenic pressure on the landscape during the Roman Empire and the Little Ice Age.

Mediterranean deltas contain a widespread and generally consistent Holocene stratigraphic succession composed of peat, lagoonal, and other organic-rich facies that accumulated as delta plain deposits at or near sea level (Stanley and Warne, 1994). These resource-rich ecosystems were used by humans soon after their development. Documented archaeological sites dated to 7000 yr BP or earlier are positioned on or adjacent to deltas, such as those of the Rhône and the Nile (Stanley and Warne, 1997).

Benthic foraminifera have been long and widely used as indicators of past environmental conditions (i.e., salinity, temperature, oxygen content, etc.) in open marine and coastal areas (Murray, 2006) and are a valuable tool, in combination with the sedimentological analysis of the stratigraphic succession and other palaeontological and geochemical proxies, for palaeoenvironmental reconstruction. However, the use of foraminifera for an accurate reconstruction of coastal habitats is not straightforward due to the enormous complexity and variability of these ecosystems. This is of paramount importance in the case of deltas because a small delta plain such as the Ebro (320 km^2) contains at least four different habitats with particular foraminiferal assemblages (Benito et al. (2005) and Tables 1 and 2). Moreover, the existing literature shows that previous palaeoenvironmental reconstructions of Mediterranean deltaic sequences have used modern analogues only from open marine environments (Amorosi et al., 1999, 2013; Rossi and Horton, 2009; Curzi et al., 2006; Carboni et al., 2010; Dinelli et al. 2012; Milli et al., 2013) and not from delta plain habitats (coastal lagoons, inner bays, salt marshes, etc.). Thus, the present study represents the first palaeoreconstruction based on both open marine and

delta plain assemblages, thereby providing the possibility for a new and sounder interpretation of the fossil record in deltaic sedimentary sequences.

Previous work

Earlier geological studies of the Ebro Delta and its Holocene sedimentary archives and evolution are scarce and most of them supported by just a few radiocarbon dates, especially initial works carried out in 1960s and 1970s (e.g., Solé et al., 1961; Macau, 1961; Maldonado and Riba, 1971; Maldonado, 1972). According to Maldonado and Murray (1975) and a sedimentological and palaeontological comparison between borehole sedimentary successions and recent environments, after a temporary stabilization of sea level at ca. -10 m extensive deltaic progradation started, and the delta plain formed over the last 8.0 ka (based on peat material radiocarbon dated by Solé et al. (1965) to 7680 yr BP). The fluvial supply of sediment was sufficient to prevent extensive transgression over the delta plain during this time interval, which was concurrent with the slowing of the sea-level rise. Maldonado and Murray (1975) concluded that the entire development of the Ebro Delta was governed mainly by the interaction between the rate of sea-level rise and the rate of sediment delivery by the river. Other factors, such as river floods and coastal processes caused the diversion of the distributaries as well as changes in the delta morphology, with river avulsions being responsible for evolution of the delta through sequential progradation and abandonment of different deltaic lobes, which were subsequently modified by rapid subsidence. Thus, the geometry of Ebro Delta was created by the advance of successive deltaic lobes that prograded radially seawards from an avulsion point usually located close to Gracia Island (Maldonado and Riba, 1971). These processes

were studied by Maldonado (1977) who found evidence for five different major avulsions during the last centuries (Díaz et al., 1990).

The Holocene deposits of the delta present a thickness ranging from 20 m on the landward side to 52 m on the delta front (Maldonado, 1972; Maestro et al., 2002). Radiocarbon ages indicate that deposition of the prodelta on the shelf began at approximately 11,000-10,000 yr BP (Díaz et al., 1990). After the pioneering work of Maldonado (1972), Somoza et al. (1998) published the most comprehensive study of the Holocene depositional units of the Ebro Delta based on high-resolution seismic profiles and analysis of 11 existing boreholes (20-60 m long) drilled on the modern delta (3 in the alluvial valley, 7 in the delta plain and 1 in the prodelta). The Holocene deposits of the delta were interpreted as a depositional sequence composed of a transgressive systems tract (TST), composed mainly of a basal mollusc-shell lag and marine grey or black clays overlying the upper Pleistocene gravels, and a highstand systems tract (HST). The top of the maximum flooding surface (MFS) separating the TST from the HST was dated to 6900 yr BP based on peat material from the inner delta area previously published by Arasa (1994), as they did not obtain any direct dates from their sedimentary sequences. The HST, which overlies the MFS, is reported to include a total of five progradational units made of prodelta clays, delta front sands or delta-plain silty sands, depending on the location within the deltaic three-dimensional architecture. Only their ITGE-6 borehole was drilled in the central area of the delta plain near Gracia Island (Figure 1). The ITGE-6 borehole was approximately 30 m long, of which approximately 27 m was Holocene in age. The Holocene stack was interpreted to be composed of five progradational units (with assigned ages in Somoza and Rodríguez-Santalla, 2014). Basal unit d0 is composed of bioclastic coarse

sand containing marine molluscs and deposited during the TST before 7000 yr BP. Units d1 and d2 are composed of coarse and medium sands that accumulated above the MFS and are dated to between 6150 and 3600 yr BP. These three lower units are considered to be delta-front and nearshore deposits. Finally, units d3 and d4 are characterized by sands with scattered pebbles and silty sands, which are defined as delta-plain deposits younger than 2700 yr BP. These progradational units were interpreted to have been deposited as a succession of prograding delta lobes with frequencies of on the order of thousands of years.

Canicio and Ibáñez (1999) identified several coastal barriers separating thick peat bodies in the landward limit of the present delta plain dated to 3050±45 radiocarbon years in the northern hemidelta and 5745±50 radiocarbon years in the southern hemidelta. They concluded that the orientation of the barriers suggests that at approximately 6000 yr BP the mouth of the delta was near the present fluvial island of Gracia (Figure 1).

Recently, in contrast to the above-mentioned studies, Maselli and Trincardi (2013) supported the idea that Amposta, a town now located at the inland margin of the delta, had a marine harbour during Roman times. This erroneous idea began with a personal interpretation of Roman texts by Bayerri (1934) who considered the mention of a “sea port” in Tortosa (12 km upstream of Amposta; Figure 1) to be proof of the existence of an estuary. The concept of “sea port”, however, could also refer to fluvial ports that harbour marine vessels. As noted by Canicio and Ibáñez (1999), the same misinterpretation led some other authors to consider that the Ebro Delta formed very recently (mostly during the Islamic Period in the 14th and 15th centuries) and that it was an estuary during Roman times. For example, Guillén and Palanques (1997) and

Palanques and Guillén (1998) considered that the Holocene sea-level rise caused the flooding of the river mouth, which became an estuary that evolved into a delta only during the last 2.0 ka. Some publications even concluded that the delta plain began to form during the 12th century downstream from the town of Amposta (Serra, 1997; Somoza and Rodríguez-Santalla, 2014).

Successive delta lobe progradation has been identified during the last millennium in the Ebro Delta through the recognition of three main lobes: the Riet Vell, Riet de Zaida and Migjorn lobes (Ibáñez et al., 1997) (Figure 1). The oldest map showing a relatively detailed and reliable configuration of the Ebro Delta is the Mercator-Hondius Atlas, which dates from 1580 CE (Ibáñez et al., 1997). The southeastern Riet Vell lobe was the main active mouth of the delta in 1149 CE and was probably abandoned in 1362 CE (Somoza and Rodríguez-Santalla, 2014). Modern bathymetric configuration suggests that partial marine destruction of this abandoned lobe provoked an 8 km retreat of the old headland and the subsequent growth of the southern La Banya spit (Canicio and Ibáñez, 1999). After this period, the main mouth of the Ebro Delta moved northward to the Riet de Zaida lobe, which was already active in 1575 CE (Somoza and Rodríguez-Santalla, 2014). This lobe was separated from the old Riet Vell lobe by a large palaeobay (Port Fangós), and it developed from the proximal zone of the delta, suggesting that it was built by the switching of the river near the Gracia Island (Figure 1). This new channel, shorter and with a larger hydraulic gradient to the sea, provoked a quick decay of the old Riet Vell main channel. The next detailed maps include a navigation chart of the Ebro Delta coast (Plan Des Rades de Sausa, 1733 CE) and the map of Miguel Marín (1749 CE) (Canicio and Ibáñez, 1999). The main differences with the previous situation at the

end of the 16th century were the complete filling of the palaeobay that separated the two previous deltaic lobes and the rapid progradation of the new and central Migjorn lobe. This last active lobe was the result of a river switching event that took place in approximately 1666 CE at a location called La Cava near Gracia Island (Figure 1) as a consequence of a reported anthropogenic excavation in the outer levee of a pronounced meander (Ribas, 1996). The retreat of the Riet de Zaida lobe by marine erosion led to the subsequent development of the Fangar spit that started to form in approximately 1739 CE, as indicated on the Miguel Marín map (Canicio and Ibáñez, 1999). Modern maps show a rapid progradation of the central Migjorn lobe until 1880 CE due to the filling of the shallow inner palaeobay of Port Fangós, followed by a shift of the delta mouth during the 1930s and a quick retreat during the last decades due to sediment retention in the various dams located along the Ebro River watercourse (Ibáñez et al., 1997).

Another controversial issue related to the hypothesis of a recent and rapid growth of the Ebro Delta is the impact of land use changes in the river basin on the progradation rates. The 13th century is considered to be the beginning of intense deforestation in the Ebro basin due to changes in land use from forest to agricultural activities. These changes favoured sediment erosion and may have caused significant progradation of the Ebro River mouth (Palanques and Guillén, 1998; Maselli and Trincardi, 2013; Somoza and Rodríguez-Santalla, 2014). However, a recent study modelling sediment transport in the Ebro River during the last 4.0 ka (Xing et al., 2014) shows that sediment load was already high (30.5 Mt yr^{-1}) before any significant human intervention and that the increase in sediment load due to land use change was up to a maximum of 47.2 Mt yr^{-1}.

Modern foraminifera (live and dead assemblages) off the Ebro Delta were studied extensively by Scrutton (1969), who quantitatively defined the different species that characterized mainly the open marine environments. In contrast, the study of delta plain habitats was very limited (only 6 samples from a coastal lagoon). Afterwards, Maldonado (1972) published qualitative results on the presence of benthic foraminifera in several surface (total assemblages) and borehole samples from the Ebro Delta (from both delta plain and open marine environments). More recently, an exhaustive analysis of delta plain and nearshore foraminiferal assemblages of the Ebro Delta was carried out by the authors (see Tables 1 and 2), which complements very well the study by Scrutton (1969). Data from both studies are the basis for the palaeoreconstruction conducted in the present paper, in combination with the interpretation of stratigraphic sequences and radiocarbon dates. The geological analysis of continuous borings from deltas and their lateral correlations can define the associated environments of deposition. Such analyses provide a context for interpreting both regional palaeogeography and site-specific environmental settings.

Objectives

The present work is focused on the methodological contribution of foraminiferal assemblages to reconstructing the sequence of palaeoenvironments that characterize the Holocene evolution of the central Ebro Delta plain. We supply new data to pinpoint the age of the delta, as it has been questioned in recent years (Maselli and Trincardi, 2013). We contribute substantial new environmental and chronological information to complete and improve previous interpretations (e.g., Somoza et al., 1998).

The main aim of the current work is to provide new insights into the Holocene evolution of the Ebro Delta using micropalaeontological proxies (benthic foraminifera) based on modern analogues covering the whole range of deltaic environments (from the inner delta plain to the outer prodelta).

The combination of the fossil foraminiferal data obtained from two new boreholes with the available geological knowledge (mainly published by Somoza et al, 1998) and the existing data of modern foraminifera allowed a more precise reconstruction of deltaic environments and their evolution through time in the central delta-plain area. From this knowledge, a new understanding of some controversial points regarding the origin and evolution of the delta has been obtained. In addition, numerous radiocarbon dates allowed a detailed chronology of the deltaic successions in the two boreholes to be made.

Materials and methods

Study area

The Ebro Delta is one of the largest modern deltas in the Mediterranean after those of the Nile, Rhône and Po (Barnolas et al., 1996). It is located on the western Mediterranean coast, approximately 200 km southwest of Barcelona, and it extends over an area of 320 km^2. It has an outer sandy shoreline 50 km long and an estimated sedimentary volume of 28 km^3 (Figure 1). The maximum tidal amplitude is 0.25 m (astronomical) and 1 m (meteorological) (Sánchez-Arcilla et al., 1996; Somoza and Rodríguez-Santalla, 2014).

The main morphological features of this microtidal delta are two spits, Fangar and La Banya, which partially close two adjacent bays, Fangar and Alfacs (Figure 1).

Most of the surface area of the modern Ebro Delta has been devoted to agriculture since the construction in 1860 CE of the first irrigation canal, which transformed most wetlands and some lagoons into rice fields, which occupy 65% of the delta plain (Cardoch et al., 2002; Ibáñez et al., 2010; Roca and Villares, 2012). Natural delta habitats account for only 20% of the surface area and include freshwater, brackish and saline lagoons, salt marshes and coastal and sandy dune systems (Valdemoro et al., 2007). Several national and international designations (RAMSAR, Natura 2000 and Natural Park) currently protect the natural delta habitats.

At present, RSLR and coastal erosion by wave action cannot be compensated by river sediment input (Ibáñez et al., 1997; Jiménez et al., 1997). A series of dams were built along the Ebro River watercourse mainly in the 1960s to support a variety of intensive water uses (Ibáñez and Prat, 2003). Irrigation and damming are responsible for a 30% decrease in the water discharge, and the reservoirs retain approximately 99% of the sediment input that would otherwise be partially deposited in the Ebro Delta, creating a severe sediment deficit (Ibáñez et al., 1996). As a result, the delta has ceased to grow, erosive processes are dominant, and it has changed from progradational to a storm wave-dominated coast that is being morphologically reshaped (Guillén and Palanques, 1992; Jiménez and Sánchez-Arcilla, 1993; Jiménez et al., 1997).

At different temporal scales, Somoza et al. (1998) estimated subsidence rates of approximately 1.75 mm/yr for the Ebro Delta during the last 7.0 ka, and Ibáñez et al. (1997) considered a subsidence of 2 mm/yr for the last 0.3 ka and recent subsidence rates to be 1-3.2 mm/yr. Recent research combining subsidence and sea-level rise data

along the Ebro Delta coast estimate a variable RSLR ranging between 2 and 6 mm/yr (Jiménez et al., 1997), and from 4 to 6 mm/yr (Ibáñez et al., 1997).

Sampling

The Carlet and Sant Jaume boreholes were drilled in 2011 in reclaimed areas of the central modern delta plain (Figure 1). The Carlet borehole is located at X 303479/Y 4508218, approximately 18 km from the modern delta mouth, and it is Z 2.33 m above the national ordnance datum and 19.27 m long. The Sant Jaume borehole is located at X 310438/Y 4508070, approximately 10.5 km from the modern delta mouth, and it is Z 1.02 m above the national ordnance datum and 21.95 m long. The depths are always referred to the Spanish national ordnance datum (mean sea level at Alicante recorded between 1870-1882 CE). The boreholes did not reach the basal Pleistocene gravels, although some gravels were recovered in Carlet, suggesting their proximity. They were drilled using a percussion/rotary drill that produced a core approximately 8 cm in diameter. The cores comprise alternating sands, sandy muds, muddy sands and muds with plant remains and mollusc-shell fragments in the muddy and sandy intervals.

Analyses

Foraminifera. Samples for micropalaeontological analysis were taken from the boreholes at approximately 25-cm (Carlet) and 20-cm (Sant Jaume) intervals. They were dried in an oven at 50°C and weighed. The target weight was 70 g per sample. Samples were wet sieved through 63-micron and 2-mm meshes to retain sand and gravel respectively. The samples were then dried and weighed again to determine the proportion of sand. The foraminifera were concentrated using trichloroethylene. Samples were split into fractions using a splitter, and tests were picked until a

representative amount of more than 300 individuals for each assemblage was obtained. Otherwise, all the available tests were picked and studied under a stereoscopic binocular microscope using reflected light. Only assemblages with more than 100 tests were used for calculations. Altogether, 143 samples were studied (Table S1), and more than 21,850 foraminifera grouped into 113 different species were identified (Appendix A).

The species were divided into deltaic and marine forms based on modern distributions and abundance of living foraminiferal assemblages in the Ebro Delta environments based on a quantitative study by Scrutton (1969) and our own data (Table 1). Dead foraminiferal assemblages were also characterized from modern samples and the results used as modern analogues for the interpretation of the fossil foraminiferal record (Table 2).

Radiocarbon dating. Thirty-nine samples of shell fragments and three samples of wood were radiocarbon dated. Radiometric analyses were carried out by Beta Analytic Inc. (Miami, USA) and NOSAMS (Woods Hole, USA) using Accelerator Mass Spectrometry (AMS). The radiocarbon ages of shells were adjusted for the marine reservoir with a local deltaR correction, and conversion of all dates into calendar years was performed using 2013 calibration databases (Reimer et al., 2013) (Table 3).

Statistical analyses. Fisher's alpha index was calculated for foraminiferal assemblages with >100 tests (Murray, 2006) to explore their diversity. Based on the alpha values, a clear boundary can be drawn between normal marine environments (alpha >5) and restricted marginal marine environments (alpha <5).

A Detrended Correspondence Analysis (DCA) was used to determine whether fossil foraminiferal assemblages were represented by the modern Ebro Delta habitats.

This was performed by passively plotting onto the same unconstrained ordination space modern (dead) foraminiferal samples along with the borehole samples. Analyses were performed using the '*vegan'* package of R (Oksanen et al., 2013).

The Linear Discriminant Function (LDF) technique was used to statistically assign each fossil sample to the most likely modern habitat group. A total of four modern habitat groups based on cluster analyses of dead foraminiferal samples were identified in the Ebro Delta: 1) offshore, 2) nearshore and outer bays, 3) coastal lagoons and inner bays, and 4) salt and brackish marshes. The LDFs estimated the probability (0–1) that a borehole sample should be classified into each of the four modern habitat groups by means of discriminant functions. The relative abundances of the foraminiferal data were square root transformed prior to the analyses to stabilize their variance. Following Kemp et al. (2012), samples with probabilities of >0.95 are considered exclusive to one habitat group, whereas those with probabilities of <0.95 samples can be assigned to more than one group. The LDFs analyses were carried out using the '*MASS'* package of R (Venable and Ripley, 2002).

The Modern Analogue Technique (MAT) was used to test the reliability of the palaeowater depth reconstructions based on the transfer function developed by the authors. This technique evaluates the degree of similarity (or dissimilarity) in the foraminiferal assemblages between each fossil sample and the modern assemblages. The squared chord distance (SCD) was used as dissimilarity coefficient. Using the largest dissimilarity coefficient among all the modern foraminiferal samples as a critical threshold (Woodroffe, 2009), we identified fossil samples with close modern analogues. Samples with SCDs of ≤0.271 were considered similar. The MAT analyses were calculated using the '*analogue'* package of R (Simpson and Oksanen, 2014).

Results

Based on general sedimentological features (sand content), foraminiferal test abundance, and species diversity and dominance, the microfossil assemblages present in the two boreholes can be divided into different depth intervals (DIs). Table 4 and Figures 2 and 3 summarize the main borehole and microfaunal data. Interpretation of these DIs in terms of different habitats or subenvironments that evolved through time in this central area of the Ebro Delta is based on a palaeowater-depth transfer function developed by the authors. This transfer function compares the buried Holocene assemblages with dead foraminiferal assemblages in various settings of the modern delta based on data previously obtained by Scrutton (1969) and our own data (Table 2 and Figure 4).

At the base of the Carlet borehole, DI5 is composed of at least 7.5 m of muds and is characterized by an assemblage highly dominated by *Ammonia beccarii* (average 74%) and *Cribroelphidium selseyense* (13%), with minor *Quinqueloculina seminula* (4%). The number of species is moderate (average 10), and the contents of marine and porcellaneous tests are low (average 7% and 8%, respectively). The comparison with modern assemblages suggests a lagoonal or shallow inner bay environment (0.5-1.5 m depth) for this interval, which developed during a long time spam from 7600 to 2600 yr BP. Above DI5, DI4 is composed of 3.5 m of sands with variable abundances of foraminifera, and a high number of species (21), marine tests (34%) and porcellaneous forms (35%). The assemblages are composed mainly of *A. beccarii* (36%), *Q. seminula* (18%) and *C. selseyense* (13%), with secondary *Rosalina anomala* (6%), *Triloculina marioni* (6%) and *Cibicides lobatulus* (4%). All these

features indicate a sandy environment with a mixture of deltaic (inshore) and marine (offshore) species, similar to a beach or back-barrier setting around the deltaic fringe. The transfer function did not find a close modern analogue for the assemblages in this interval, although the assemblages do indicate very shallow palaeowater depths (*c*. 0–1 m). No age has been obtained in DI4 but radiocarbon ages from the underlying and overlying intervals suggest it developed after 2600 and before 2000 yr BP. Consequently, the coastline was located close to this location around this time. The overlying 3.7 m of muddy sands (DI3) contain very few foraminiferal tests and may indicate the shift to a higher elevation and less flooded habitat (an alluvial environment closer to the river levee) in the area of Carlet approximately 2000 yr BP. Subsequent conditions suggest the presence of a fresh to brackish marsh environment (less than 0.5 m depth) in which 1 m of muddy sediments (DI2) was deposited at approximately 1700 yr BP. These sediments are characterized exclusively by an abundant *A. beccarii* assemblage, and the presence of terrestrial gastropods and oogonia of characeae algae is indicative of very low salinity conditions in this area. Finally, DI1, with 2.7 m of muds, also features terrestrial gastropods and characeae oogonial, but the foraminiferal content is very low (only a few tests of *A. beccarii*), suggesting a lacustrine environment. Radiocarbon dates show a great variety of ages and inverted dates. This reinforces the idea that, during the last 2.0 ka (DI2-1), this area was a fresh to brackish aquatic environment located close to the river thus featuring a relatively high elevation and occasional marine flooding conditions.

In contrast, the Sant Jaume borehole shows much more recent and deeper materials than the Carlet borehole. The lower part of the sequence initiates with DI5 and more than 3 m of muds containing a variable abundance of foraminifera

characterized by a high number of species (22), marine tests (43%) and porcellaneous forms (24%). The assemblage is composed mainly of *C. selseyense* (18%), *A. beccarii* (13%) and *Q. seminula* (11%), together with *Cribroelphidium poeyanum* (6%), *Brizalina variabilis* (5%), *Bulimina gibba* (4%), *Valvulineria bradyana* (3%) and *Rosalina irregularis* (3%). A radiocarbon age of 1760 yr BP for the upper part of this interval indicates that in this period the sediment accumulated in the nearshore environment (approximately 7 m depth). The following unit (DI4) is represented by 6.3 m of muddy sediment deposited in an inshore more proximal setting (lagoon or shallow inner bay environment; 0.5-1.5 m depth) dominated by *A. beccarii* (65%) and *C. selseyense* (19%), with *Q. seminula* (3%) and *C. poeyanum* (3%). The number of species is moderate (13) and the marine tests (8%) and porcellaneous content (5%) are low. This interval developed between 1700 and 1100 yr BP. Above this unit, a 3.4-m unit of sandy muds with a variable abundance of foraminiferal tests exhibits an increase in the number of species (18) and marine (34%) and porcellaneous (16%) tests (DI3). An assemblage composed of *A. beccarii* (38%), *C. selseyense* (18%) and *Asterigerinata mamilla* (11%), with minor *Quinqueloculina oblonga* (3%), *Q. seminula* (3%) and *Haynesina germanica* (3%), suggests a sandier nearshore habitat (approximately 7 m depth) that developed approximately 1.0 ka ago. The overlying interval DI2 (4 m of muds) shows a decrease in the open marine influence (15% marine tests and 5% porcellaneous forms), a moderate number of species (14) and the dominance of more deltaic (inshore) forms, such as *A. beccarii* (52%), *H. germanica* (11%), *Cribroelphidium oceanensis* (11%) and *C. selseyense* (8%), with *B. variabilis* (6%). These features are indicative of a lagoonal or shallow inner bay environment (0.5-1.5 m depth) that developed in this area between 900-600 yr BP. The final 3.3 m

of sandy muds (DI1) are younger than 0.5 ka, contain few foraminiferal tests (*A. beccarii*, *H. germanica* and *C. selseyense*) and may represent an emerged fresh-water environment with occasional marine flooding located in a delta plain.

Discussion

Palaeoenvironmental evolution of the Ebro Delta

A comparison of the materials, microfossil assemblages, radiocarbon ages and palaeoenvironmental evolution of the two boreholes clearly indicates that the more landward Carlet sedimentary sequence exhibits sandier, older and more continental conditions, whereas the Sant Jaume geological record exhibits muddier, younger and more marine environmental conditions characteristic of a more seaward setting within the Holocene architecture of the Ebro Delta. These distinctive stratigraphic and foraminiferal sequences, with an older and more proximal progradational record on one side and a younger and more distal progradational record on the other side, are also found in other Mediterranean deltas, such as the Rhône (France) and the Po (Italy) (Amorosi et al., 2005, 2013; Boyer et al., 2005; Rossi and Vaiani, 2008; Dinelli et al., 2012). However, the interpretation of the environments in some cases is different than in the present study because a wider range of foraminiferal assemblages, including open marine and delta plain environments, is considered in this study (see discussion on this topic in the following section).

The palaeoenvironmental interpretation of the sedimentary sequences in the Carlet and Sant Jaume boreholes is based on diagnostic foraminiferal assemblages and is shown in Figure 5. At Carlet, apart from the lowermost part of DI5 deposited before 7.0 ka during a TST under rising sea-level conditions, the muddy DI5 at the base and

the sandy DI4 are interpreted to be mainly a part of a sequence composed of inner bay-lagoonal-beach deposits in this central area under sea-level highstand conditions between 7000 and ~2000 yr BP. Then, further sediment accumulation led to the formation of a series of non-marine deposits represented during the last 2.0 ka, initially represented by continental sands in DI3. These deposits were followed by a very low salinity marsh environment with occasional marine flooding at approximately 1700 yr BP (DI2), which was finally replaced by a fresh-water muddy environment (higher elevation and closer to the river levee) containing a mixture of materials with variable radiocarbon ages (DI1).

A comparison of the Carlet results with the previous ITGE-6 borehole sequence of Somoza et al. (1998) indicates the partial absence in our record of the most basal units of the Holocene sequence that were deposited under rapidly rising sea-level conditions (TST) (Figure 5). There are similarities but also important quantitative and qualitative differences between the two records in terms of palaeoenvironmental reconstructions and the timing of events. The lower part of our muddy DI5 interval (deposited between 7.6 and 7.0 ka) could be correlated to the muddy aggradational unit (a1) in ITGE-6 (deposited as the transgressive wedge h1 before 7.0 ka) and represents the final record of the TST. After the MFS, suggested by Somoza and Rodríguez-Santalla (2014) to have occurred at approximately 6900 yr BP, the remainder of the muddy DI5 and sandy DI4 intervals (deposited between 6.9 and 2.5 ka) could be correlated to the sandy units d1 and d2 (delta front/nearhore) in ITGE-6 (deposited between 6.1 and 3.6 ka under sea-level highstand conditions). Then, the series of delta-plain deposits (the sandy and muddy intervals DI3-DI1) during the last 2.5 ka in Carlet very likely correspond to the sandy and silty d3 and d4 delta-plain

units (considered to be younger than 2.7 ka) in the ITGE-6 sequence. However, the information provided by the foraminiferal assemblages in our study suggests that the maximum Holocene marine transgression did not reach the inner part of the Ebro Delta in the form of open-sea environments but rather via lagoon and/or shallow bay development. This is an important difference with the interpretation provided by Somoza et al. (1998) in relation to the existence of a transgressive wedge (h1) with marine clayey sediments corresponding to the MFS. Our results clearly show the existence of restricted and brackish environments, which is more compatible with the presence of fresh-water peat deposits in the innermost part of the delta during that time (Solé et al., 1961; Arasa, 1994), because fresh-water peat cannot form during high-salinity conditions. This reasoning also applies to the other highstand sea-level events (h2, h3, and h4) postulated by Somoza et al. (1998) in the innermost part of the delta (upstream of the city of Amposta in the alluvial valley) and next to the Ebro River, where each period of fresh-water peat accumulation would coincide with the presence of the salt-water conditions. We do not find any evidence for this interpretation, and an alternative explanation is a succession of fresh-water peat deposits and alluvial or lagoonal deposits as a function of the changing distance between the borehole location and the Ebro River through time (due to the migration of the river course), as well as changes in the frequency and magnitude of river floods.

This alternating pattern of peat and alluvial or lagoonal clay deposits is also found in the innermost part of other large Mediterranean deltas. In the Po delta plain, Amorosi et al. (2005) describe a similar sequence in the innermost boreholes (204-S17, 204-S5, 204-S6) with the presence of peat layers in the middle of fresh-water (swamp) clays or brackish-water (lagoonal) clays, whereas the marine (bay) clays are

only found in the outermost boreholes (204-S7, 205-S5) and never coincide in time with peat layers. This study also included the analysis of microfossils (foraminifera and ostracoda) and similar foraminiferal assemblages (Ba-Bd) with few species that were interpreted as low-energy brackish-water back-barrier environments. In the Rhône Delta, Boyer et al. (2005) also describe the presence of clay (including layers of alluvial sand) with brackish to fresh-water fauna in the innermost boreholes (109, 108, 126), whereas clays with marine fauna are only found in the outermost boreholes (125 to 106).

The Sant Jaume borehole is located in a more seaward position than Carlet and contains a longer, deeper and much younger sequence that accumulated during the last 2.0 ka. Due to the available historical data discussed above, it is possible to interpret its sedimentary record as deposition during the formation and development of three different deltaic lobes under highstand sea-level conditions. The muddy intervals DI5 and DI4 represent a partial record of the formation and development of the Riet Vell lobe that prograded towards the southeast and deposited progressively shallower (from nearshore to more proximal inner bay) materials in this area between 2000 and 1100 yr BP. Then, deposition of a new muddy progradational shallowing-upward succession between 1100 and 500 yr BP, represented by DI3 and DI2, characterizes the development of a new deltaic lobe (Riet de Zaida) that developed towards the northeast and deposited nearshore-inner bay-lagoonal sediments in this area. A more recent switch in the river course due to human intervention created the newest delta lobe (Migjorn) represented by lacustrine (fresh-water) deposition (DI1) in this area during the last 0.5 ka.

Two external boreholes (ITGE-1 and ITGE-2; Figure 1) were studied by Somoza et al. (1998), although their descriptions are less detailed than the central ITGE-6 borehole. Both sedimentary successions reached the Pleistocene gravels, were approximately 50 m thick, and included TST and HST deposits. The HST was composed of four progradational units (dl, d2, d3 and d4) and three aggradational units (a2, a3 and a4). The boreholes were located at the apices of two main delta lobes identified in historical records: ITGE-l over the Riet Vell lobe, and ITGE-2 over the most recent Migjorn lobe. Their final progradational unit (d4) corresponds to the formation of their respective deltaic lobes, but no information on the origin, sedimentary characteristics and chronology of the other earlier progradational units is presented. Our Sant Jaume borehole is located in the central delta plain at the confluence area of the last three delta lobes: Riet Vell, Riet de Zaida and Migjorn (Figure 1). Distinct marine and delta plain habitat successions have characterized the formation and development of those three lobes, and these habitat successions were associated with particular foraminiferal palaeoassemblages. First, progradation of the Riet Vell lobe (2.0-1.1 ky) resulted in progressively shallower muddy environments from nearshore (DI5) to more proximal inner bay (DI4). The Riet de Zaida lobe (1.1-0.5 ky) exhibits a similar environmental succession with nearshore (D3) and inner bay-lagoonal sediments (DI2). Finally, the most recent Migjorn lobe (0.5 ka) is represented by a fresh-water environment (DI1) in a delta plain setting.

As we have shown, important difference exist in the scale of resolution between the Carlet and Sant Jaume boreholes. Carlet provides information at a temporal resolution of thousands of years, whereas San Jaume provides data at the historical scale. A similar thickness of sediments represents 7.6 ka in Carlet and circa 2 ka in

San Jaume. The Carlet borehole correlates with the progradational d1, d2, d3 and d4 of Somoza et al. (1998), which correspond to four different 5th-order cycles. In contrast, the entire record of the San Jaume borehole can be assigned to the prograding portion of one complete cycle of higher rank, corresponding to the last d4 unit of the historical lobes Riet Vell, Riet de Zaida and partially the d5 unit of Migjorn. In addition to the processes of compaction, preservation and possible time-averaging experienced by the older Carlet sedimentary sequence, the shorter time interval and deeper environments represented by the longer Sant Jaume sedimentary sequence can be understood as a consequence of the greater accommodation space available in the delta seaward from Gracia Island. As shown in Figure 5A, the geometry of the Holocene materials has a thickness ranging from 20 m on the landward side (Amposta) to 52 m at the delta front. The erosional unconformity between the upper Pleistocene gravels and the Holocene deposits exhibits a more pronounced slope in the external delta just beyond Gracia Island and was formed initially by marine erosion during rapid sea-level rise during the first stages of the Holocene transgression (Maestro et al., 2002). These authors also indicated the presence of extensional tectonics that affected the Quaternary deltaic deposits via the formation of large-scale faulting that generated differential subsidence beneath the Ebro Delta and increased the slope angle. The principal process involved in fault development is considered to be differential compaction resulting from the prograding deltaic lobes that overlie aggradational clay deposits. Growth faults increase subsidence, which in turn generates accommodation space for subsequent prograding deltaic sediment. This arc-shaped topographic depression acted as a trap for distributary channels meandering across the delta plain, such as the abandoned Riet Vell and Riet de Zaida (Maestro et al., 2002).

Implications for the Holocene evolution of Mediterranean deltas

In terms of their palaeoenvironmental significance, when modern foraminiferal assemblages from the delta plain habitats are included in the analysis, the interpretation is more robust compared with other studies that only consider open marine (offshore) assemblages. The existing literature shows that foraminiferal assemblages living in coastal marginal environments, such as coastal lagoons, bays or salt marshes, differ greatly from those in adjacent offshore habitats (Murray, 2006). This also applies to some worldwide and Mediterranean deltas, such as the Mississippi, USA (Lankford, 1959), Mahakam, Indonesia (Lambert, 2003), Rhône, France (Vangerow, 1974; Fanget et al., 2012), Nile, Egypt (Arbouille and Staney, 1991) and Ebro, Spain (Scrutton, 1969). Previous studies often interpreted the occurrence of shallow brackish-marine species, such as *Ammonia* spp. (*A. tepida, A. beccarii, A. parkinsoniana*), *Cribroelphidium* spp. and/or *H. germanica*, as indicators of past offshore habitats within Holocene deltaic sequences (Amorosi et al., 2008, 2013; Rossi and Vaiani, 2008; Milli et al., 2013). However, it is well known that these species are mainly indicative of particular marginal coastal habitats, unless other ecological requirements based on the study of their living populations are actually identified (Usera et al., 2002; Guillem, 2007). Otherwise, the lack of close modern analogues may lead to weaker interpretations of the foraminiferal fossil record.

The present study has demonstrated the similarity between most modern and fossil samples in the Ebro Delta by applying the modern analogue technique (MAT) and Linear Discriminant Functions (LDFs). Hence, a finer-grained habitat reconstruction can be achieved. The interpretation of results would have been different if foraminifera from deltaic (inshore) environments had not been included, especially

for the Carlet sequence, which features the presence of shallower habitats typical of delta plain environments, in comparison with the Sant Jaume sequence, which features deeper environments typical of the prodelta and delta front. To our knowledge, this is the first attempt to include modern samples from both delta plain (coastal lagoons, marshes and inner bays) and open marine (prodelta and delta front) habitats of a Mediterranean delta to provide adequate analogues for all borehole samples. Thus, the Ebro Delta data set could be used in other Mediterranean deltas with the aim to provide new interpretations of their depositional environments because all of these deltas share a similar Holocene evolution (Stanley and Warne, 1994).

The application of a water depth transfer function to fossil foraminiferal assemblages has complemented the palaeoenvironmental reconstruction of the Ebro Delta. The only comparable work is by Rossi and Horton (2009), who applied the Northern Adriatic Transfer Function (NATF) to reconstruct the evolution of the Holocene palaeobathymetry of the Po Delta. These authors concluded the existence of a shallowing upward trend following the progradational succession of this delta during the last 5.5 ka. In turn, the palaeowater depths were considered reliable according to MAT results. For the Ebro Delta, very similar results were found in the Sant Jaume sequence, where two deeper-to-shallower successions were detected (DI5-4 and DI3-2) with inferred water depths from 7 to 1 m (Figure 5). These findings suggest the progradation of delta lobes in this distal part of the delta during the last centuries, although some samples did not contain close modern analogues. In contrast, the palaeowater depths of the Carlet sequence revealed very shallow conditions throughout all of the recorded depositional environments, with water depths ranging from 1–2 m. The validity of these reconstructions is supported by the MAT and LDF

results, although palaeowater depths must be taken with caution because of the complex relationships between water depth and foraminiferal distributions, particularly in highly dynamic systems such as deltas. Further research on modern foraminiferal assemblages in inshore habitats of other Mediterranean deltas could allow a more reliable interpretation of their Holocene evolution.

Conclusions

The scarcity of previous geological studies and the few available radiocarbon dates from Holocene sedimentary archives, together with misinterpretations of historical documents, have permitted the idea that the present Ebro Delta plain formed mostly during the 14th and 15th centuries and that it was an estuary during Roman times. Our results support an early Holocene start for the Ebro Delta, proving that a deltaic depositional system was present throughout the Holocene and that the Ebro Valley never became an estuary. This brings the Ebro evolution story in line with other major deltas along the Mediterranean Sea and worldwide, which initiated 8.0-6.0 ka ago when the rate of fluvial sediment input overtook the decreasing rate of sea-level rise.

The palaeonvironmental evolution of the central plain of the Ebro Delta during the Holocene was reconstructed using micropalaeontological analysis of two continuous boreholes (Carlet and Sant Jaume). Diagnostic foraminiferal assemblages and the application of a palaeowater-depth transfer function allowed the definition of various lithofacies and associated environments of deposition. The geometry of the Ebro Delta was created by the advance of successive deltaic lobes, which prograded radially across the inner shelf up to 25 km seaward during the Holocene. Avulsion and channel abandonment processes are considered to be the main delta constructional

processes, with the resulting deposits subsequently being modified by rapid subsidence.

The similarity between most modern and fossil samples in the Ebro Delta has been demonstrated by applying the modern analogue technique (MAT) and Linear Discriminant Functions (LDFs), allowing a much better habitat reconstruction to be achieved. The importance of extensive characterization of modern foraminiferal assemblages from both deltaic inshore and offshore environments in order to provide adequate analogues for the interpretation of borehole samples is demonstrated particularly by the more landward Carlet sequence, which only contains shallow and inshore deltaic habitats. The palaeowater depths revealed very shallow conditions for all depositional environments, ranging from 1–2 m during the last 7.6 ka under salty, brackish and fresh-water conditions.

Acknowledgements

Microfossil samples from the Carlet borehole were prepared and analyzed initially by Alfonso Palazuelos as part of his MSc dissertation (academic year 2012/13) at the University of the Basque Country UPV/EHU. Dr. Francisco Fatela (University of Lisbon, Portugal) and an anonymous reviewer greatly improved the original manuscript with their critical comments and suggestions. It represents a contribution to the INQUA Commission of Coastal and Marine Processes and Contribution #24 of the Geo-Q Zentroa Research Unit (Joaquín Gómez de Llarena Laboratory).

Funding

Drilling and coring was funded by the US National Science Foundation grant EAR-0952146. Work on the cores presented in this study was partially financed by the Formation and Research Unit in Quaternary: Environmental Changes and Human Fingerprint (UPV/EHU, UFI11/09) and HAREA-Coastal Geology Research Group (Basque Government, IT767-13) projects. It was supported by an IRTA-URV-Santander fellowship to Xavier Benito through "BRDI Trainee Research Personnel Programme funded by University of Rovira and Virgili R+D+I projects" and the European Community's 7th Framework Programme through the grant to Collaborative Project RISES-AM-, Contract FP7-ENV-2013-two-stage-603396.

References

Amorosi A, Centineo M, Colalongo M et al. (2005) Millennial-scale depositional cycles from the Holocene of the Po Plain, Italy. *Marine Geology* 222: 7-18.

Amorosi A, Colalongo M, Pasini G et al. (1999) Sedimentary response to Late Quaternary sea-level changes in the Romagna coastal plain (northern Italy). *Sedimentology* 46: 99-121.

Amorosi A, Dinelli E, Rossi V et al. (2008) Late Quaternary palaeoenvironmental evolution of the Adriatic coastal plain and the onset of Po River Delta. *Palaeogeography, Palaeoclimatology, Palaeoecology* 268: 80-90.

Amorosi A, Rossi V and Vella C (2013) Stepwise post-glacial transgression in the Rhône Delta area as revealed by high-resolution core data. *Palaeogeography, Palaeoclimatology, Palaeoecology* 374: 314-326.

Anthony EJ, Marriner N and Morhange C (2014) Human influence and the changing geomorphology of Mediterranean deltas and coasts over the last 6000 years: From progradation to destruction phase? *Earth-Science Reviews* 139: 336-361.

Arasa A (1994) *Estratigrafia i sedimentologia dels materials Plio-Quaternaris del Baix-Ebre i sectors adjacents*. PhD Thesis, University of Barcelona, Spain.

Arbouille D and Stanley DJ (1991) Late Quaternary evolution of the Burullus lagoon region, north-central Nile delta, Egypt. *Marine Geology* 99: 45-66.

Barnolas A, Somoza L, Martín-Alfageme S et al. (1996) Estudio geológico del Delta del Ebro. Proyecto para la evaluación de la tasa de subsidencia actual (Convenio CEDEX-ITGE 6/2/1995). Report, Instituto Tecnológico GeoMinero de España, Spain.

Bayerri E (1934) *Historia de Tortosa y su comarca*. Tortosa: Moderna de Alguerri.

Benito X, Trobajo R, Ibáñez, C et al. (2015) Benthic foraminifera as indicators of habitat change in anthropogenically impacted coastal wetlands of the Ebro Delta (NE Iberian Peninsula). *Marine Pollution Bulletin* 101: 163-173.

Boyer J, Duvail C, Le Strat P et al. (2005) High resolution stratigraphy and evolution of the Rhône delta plain during Postglacial time, from subsurface drilling data bank. *Marine Geology* 222: 267-298.

Canicio A and Ibáñez C (1999) The Holocene evolution of the Ebre delta, Catalonia, Spain. *Acta Geographica Sinica* 54: 462-469.

Carboni MG, Bergamin L, Di Bella L et al. (2010) Palaeoenvironmental reconstruction of late Quaternary foraminifera and molluscs from the ENEA borehole (Versilian plain, Tuscany, Italy). *Quaternary Research* 74: 265-276.

Cardoch L, Day JW and Ibáñez C (2002) Net primary productivity as an indicator of sustainability in the Ebro and Mississippi deltas. *Ecological Applications* 12: 1044-1055.

Curzi PV, Dinelli E, Lucchi MR et al. (2006) Palaeoenvironmental control on sediment composition and provenance in the late Quaternary deltaic successions: a case study from the Po delta area (Northern Italy). *Geological Journal* 41: 591-612.

Day J, Ibáñez C, Scarton F et al. (2011) Sustainability of Mediterranean deltaic and lagoon wetlands with sea-level rise: the importance of river input. *Estuaries and Coasts* 34: 483-493.

Díaz JI, Nelson CH, Barber JH et al. (1990) Late Pleistocene and Holocene sedimentary facies on the Ebro continental shelf. *Marine Geology* 95: 333-352.

Dinelli E, Ghosh A, Rossi V et al. (2012) Multiproxy reconstruction of Late Pleistocene-Holocene environmental changes in coastal successions: microfossil and geochemical evidences from the Po Plain (Northern Italy). *Stratigraphy* 9: 153-167.

Evans G (2012) Deltas: the fertile dustbins of the continents. *Proceedings of the Geologists' Association* 123: 397–418.

Fanget AS, Bassetti MA, Arnaud M et al. (2012) Historical evolution and extreme climate events during the last 400 years on the Rhône prodelta (NW Mediterranean). *Marine Geology* 346: 375-391.

Fatorić S and Chelleri L (2012) Vulnerability to the effects of climate change and adaptation: The case of the Spanish Ebro Delta. *Ocean & Coastal Management* 60: 1-10.

Galloway WE (1975) Process framework for describing the morphologic and stratigraphic evolution of deltaic depositional systems. In: Broussard ML (ed) *Deltas, models for exploration*. Houston: Houston Geological Society, pp 87-98.

Giosan L, Syvitski J, Constantinescu S et al. (2014) Protect the world's deltas. *Nature* 516: 31-33.

Guillem J (2007) *Tafonomía, taxonomía y ecología de los foraminíferos de la Albufera de Torreblanca*. PhD Thesis, Universitat de Valencia, Spain.

Guillén J and Palanques A (1992) Sediment dynamics and hydrodynamics in the lower course of a river highly regulated by dams: the Ebro river. *Sedimentology* 39: 567-579.

Guillén J and Palanques A (1997) A historical perspective of the morphological evolution in the lower Ebro river. *Environmental Geology* 30: 174-180.

Ibáñez C, Canicio A, Day JW et al. (1997) Morphologic development, relative sea level rise and sustainable Management of water and sediment in the Ebre Delta, Spain. *Journal of Coastal Conservation* 3: 191-202.

Ibáñez C and Prat M (2003) The environmental impact of the Spanish National Hydrological Plan on the lower Ebro river and delta. *International Journal of Water Resources Development* 19: 485-500.

Ibáñez C, Prat N and Canicio A (1996) Changes in the hydrology and sediment transport produced by large dams on the lower Ebro river and its estuary. *Regulated Rivers: Research and Management* 12: 51–62.

Ibáñez C, Day JW and Reyes E (2014) The response of deltas to sea-level rise: Natural mechanisms and management options to adapt to high-end scenarios. *Ecological Engineering* 65: 122-130.

Ibáñez C, Sharpe PJ, Day JW et al. (2010) Vertical accretion and relative sea level rise in the Ebro delta wetlands (Catalonia, Spain). *Wetlands* 30: 979–988.

IPCC (2014) *Climate Change 2013: the Physical Science Basis. Working Group 1 Contribution to the Fifth Assessment Report of the International Panel on Climate Change*. New York: Cambridge University Press.

Jiménez JA and Sánchez-Arcilla A (1993) Medium-term coastal response at the Ebro delta, Spain. *Marine Geology* 114: 105-118.

Jiménez JA, Sánchez-Arcilla A, Valdemoro HI et al. (1997) Processes reshaping the Ebro delta. *Marine Geology* 144: 59-79.

Kemp AC, Horton BP, Vann DR et al. (2012) Quantitative vertical zonation of salt-marsh foraminifera for reconstructing former sea level, an example from New Jersey, USA. *Quaternary Science Reviews* 54: 26-39.

Lambeck K and Purcell A (2005) Sea-level change in the Mediterranean Sea since the LGM: model predictions for tectonically stable areas. *Quaternary Science Reviews* 24: 1969-1988.

Lambert B (2003) Micropaleontological investigations in the modern Mahakam delta, East Kalimantan (Indonesia). *Carnets de Géologie/ Notebooks on Geology Article* 2003/02.

Lankford RR (1959) Distribution and ecology of foraminifera from east Mississippi Delta margin. *AAPG Bulletin* 43: 2068-2099.

Macau F (1961) Contribución al estudio del Cuaternario en el Delta del Ebro. *Boletín de la Real Sociedad Española de Historia Natural* 59: 69-76.

Maestro A, Barnolas A, Somoza L et al. (2002) Geometry and structure associated to gas-charged sediments and recent growth faults in the Ebro Delta (Spain). *Marine Geology* 186: 351-368.

Maldonado A (1972) E1 Delta del Ebro. Estudio sedimentológico y estratigráfico. *Boletín de Estratigrafía de la Universidad de Barcelona* 1: 1-474.

Maldonado A (1977) Introducción geológica al Delta del Ebro. *Treballs de la Institució Catalana d'Història Natural* 8: 7-45.

Maldonado A and Murray JW (1975) The Ebro delta, sedimentary environments and development, with comments on the foraminifera. In: Maldonado A (ed) *Field Guide to Trip 16. Deltas of the Northern Mediterranean Sea: The Ebro Delta*. Nice: IXth International Congress of Sedimentology, pp. 19-58.

Maldonado A and Riba O (1971) El delta reciente del río Ebro: descripción de ambientes y evolución. *Acta Geológica Hispánica* 6: 131-138.

Maselli V and Trincardi F (2013) Man made deltas. *Scientific Reports* 3 (01926): 1-7.

Milli S, D'Ambrogi C, Bellotti P et al. (2013) The transition from wave-dominated estuary to wave-dominated delta: the Late Quaternary stratigraphic architecture of Tiber River deltaic succession (Italy). *Sedimentary Geology* 284: 159-180.

Murray JW (2006) *Ecology and applications of benthic foraminifera*. Cambridge: Cambridge University Press.

Oksanen J, Blanchet F, Kindt R et al. (2013) Vegan: community ecology package. R package version 2.0-10.

Palanques A and Guillén J (1998) Coastal changes in the Ebro delta: Natural and human factors. *Journal of Coastal Conservation* 4: 17-26.

Pirazzoli PA (2005) A review of possible eustatic, isostatic and tectonic contributions in eight late-Holocene relative sea-level histories from the Mediterranean area. *Quaternary Science Reviews* 24: 1989-2001.

Reimer PJ, Bard E, Bayliss A et al. (2013) IntCal13 and Marine13 radiocarbon age calibration curves 0-50,000 years cal BP. *Radiocarbon* 55: 1869-1887.

Ribas X (1996) A propósito de La Cava. *Informatiu del Museu del Montsià* 39: 5-6.

Roca E and Villares M (2012) Public perceptions of managed realignment strategies: The case study of the Ebro Delta in the Mediterranean basin. *Ocean & Coastal Management* 60: 38-47.

Rossi V and Horton BP (2009) The application of a subtidal foraminifera-based transfer function to reconstruct Holocene paleobathymetry of the Po Delta, northern Adriatic Sea. *Journal of Foraminiferal Research* 39: 180-190.

Rossi V and Vaiani SC (2008) Benthic foraminiferal evidence of sediment supply changes and fluvial drainage reorganization in Holocene deposits of the Po Delta, Italy. *Marine Micropaleontology* 69: 106-118.

Sánchez-Arcilla A, Jiménez JA, Stive MJF et al. (1996). Impacts of sea-level rise on the Ebro Delta: a first approach. *Ocean & Coastal Management* 30: 197-216.

Scruton RC (1960) Delta building and the deltaic sequence. In: Shepard ER, Phleger EB and Van Andel TH (eds) *Recent Sediments, Northwestern Gulf of Mexico*. Tulsa: American Association of Petroleum Geologists, pp. 82-102.

Scrutton ME (1969) *The distribution and ecology of recent foraminiferida off the Ebro delta, northeastern Spain*. PhD Thesis, University of Bristol, UK.

Serra J (1997) El sistema sedimentario del Delta del Ebro. *Revista de Obras Públicas* 3308: 15-22.

Simpson G and Oksanen J (2014) Analogue: Analogue matching and Modern Analogue Technique transfer function models. R package version 0.16-0.

Solé L, Macau F, Virgili C et al. (1961) *Algunos datos sobre la evolución sedimentaria del Delta del Ebro*. Madrid: Instituto de Edafología CSIC, pp. 197-199.

Solé L, Macau F, Virgili C et al. (1965). Sobre los depósitos pliocénicos y cuaternarios del bajo Ebro. *Memorias y Comunicaciones del Instituto Jaime Almera CSIC* 1: 83-92.

Somoza L, Barnolas A, Arasa A et al. (1998) Architectural stacking patterns of the Ebro delta controlled by Holocene high-frequency eustatic fluctuations, delta-lobe switching and subsidence processes. *Sedimentary Geology* 117: 11-32.

Somoza L and Rodríguez-Santalla I (2014) Geology and Geomorphological Evolution of the Ebro River Delta. In: Gutiérrez F and Gutiérrez M (eds) *Landscapes and Landforms of Spain*, Berlin: Springer, pp 213-227.

Stanley DJ and Warne AG (1994) Worldwide initiation of Holocene marine deltas by deceleration of sea-level rise. *Science* 265: 228-231.

Stanley DJ and Warne AG (1997) Holocene sea-level change and early human utilization of deltas. *GSA Today* 7: 1-7.

Usera J, Blázquez A, Guillem J et al. (2002) Biochronological and paleoenvironmental interest of foraminifera lived in restricted environments: application to the study of the western Mediterranean Holocene. *Quaternary International* 93: 139-147.

Valdemoro HI, Sánchez-Arcilla A and Jiménez JA (2007) Coastal dynamics and wetlands stability. The Ebro delta case. *Hydrobiologia* 577: 17–29.

Vangerow E (1974) Récentes observations écologiques des foraminifères dans la zone saumâtre de l'embouchure du Rhône. *Revista Española de Micropaleontología* 17: 95-106.

Vella C, Fleury T-J, Raccasi G et al. (2005) Evolution of the Rhône delta plain in the Holocene. *Marine Geology* 222-223: 235-265.

Venables WN and Ripley BD (2002) *Modern applied statistics with S*. Berlin: Springer Science & Business Media.

Woodroffe SA (2009) Recognising subtidal foraminiferal assemblages: implications for quantitative sea-level reconstructions using a foraminifera-based transfer function. *Journal of Quaternary Science* 24: 215-223.

Wright LD and Coleman JM (1973) Variations in morphology of major river deltas as functions of ocean wave and revier discharge regimes. *AAPG Bulletin* 57: 370-398.

Xing F, Kettner AJ, Ashton A et al. (2014) Fluvial response to climate variations and anthropogenic perturbations for the Ebro River, Spain in the last 4000 years. *Science of the Total Environment* 473: 20-31.

Figure and Table captions

Figure 1. Geographical location of the Ebro Delta in the western Mediterranean Sea, boreholes and places referred to in the text. Dashed line represents the approximate morphology and position of the two historical deltaic lobes (from Maldonado, 1972). Images taken from Google Earth.

Figure 2. Sedimentary sequence, sand content, general micropalaeontological data, distribution and relative abundance of the main foraminiferal species (1: *A. beccarii*; 2: *C. selseyense*; 3: *Q. seminula*; 4: *R. anomala*; 5: *T. marioni*; 6: *C. lobatulus*), and porcellaneous wall type content with depth (m) in the borehole Carlet (Ebro Delta). Foraminiferal depth intervals (DIs), radiocarbon dates (conventional years BP) and sample levels are also indicated. Black dots indicate presence of the species in assemblages with less than 100 foraminiferal tests.

Figure 3. Sedimentary sequence, sand content, general micropalaeontological data, distribution and relative abundance of the main foraminiferal species (1: *A. beccarii*; 2: *C. selseyense*; 3: *Q. seminula*; 4: *C. oceanensis*; 5: *H. germanica*; 6: *A. mamilla*; 7: *Q. oblonga*; 8: *B. variabilis*; 9: *B. gibba*; 10: *C. poeyanum*; 11: *V. bradyiana*; 12: *R. irregularis*), and porcellaneous wall type content with depth (m) in the borehole Sant Jaume (Ebro Delta). Foraminiferal depth intervals (DIs), radiocarbon dates (conventional years BP) and sample levels are also indicated. Black dots indicate presence of the species in assemblages with less than 100 foraminiferal tests.

Figure 4. Reconstruction of palaeowater-depth (associated errors as grey envelope) and different environmental settings through time in the Carlet and Sant Jaume boreholes (Ebro Delta) based on the transfer function developed by the authors. Habitat assignments using Linear Discriminant Functions (LDFs) are also shown. The foraminiferal depth intervals (DIs), number of tests and radiocarbon dates (conventional years BP) are also indicated. On the right, core trajectories projected onto DCA along with modern (dead) foraminiferal assemblages are shown. Dashed lines in DCA plots encompass modern habitat samples of each habitat type identified in the Ebro Delta: A) offshore; B) nearshore and outer bays, C) coastal lagoons and inner bays; and D) salt and brackish marshes. Water depth (m) intervals are marked for each DCA plot.

Figure 5. A. General location of the analyzed boreholes in the framework of the Ebro Delta architecture proposed by Somoza et al (1998) for the Late Quaternary; B. Palaeoenvironmental interpretation of the Carlet and Sant Jaume boreholes based on foraminiferal assemblages. Foraminiferal depth intervals (DIs), lithology and radiocarbon dates (conventional years BP) are also indicated. Interpretation of the ITGE-6 borehole is from Somoza et al (1998) with indication of the aggradational marine (a units) and progradational deltaic (d units) deposits. Dates in parentheses were assigned by Somoza and Rodríguez-Santalla (2014) but were not obtained from materials of this borehole.

Table 1. Living foraminiferal species found in and off the Ebro Delta. Above: Quantitative summary of living foraminiferal assemblages composition in different

environmental settings of the modern Ebro Delta. Figures represent relative abundance (%) unless otherwise indicated. The single value represents the average and those in parentheses give the range; Below: Reference list of marine species found in the modern foraminiferal assemblages of the Ebro Delta.

Table 2. Dead foraminiferal species found in and off the Ebro Delta. Quantitative summary of dead foraminiferal assemblages composition in different environmental settings of the modern Ebro Delta. Figures represent relative abundance (%) unless otherwise indicated. The single value represents the average and those in parentheses give the range.

Table 3. Radiocarbon dates from the Carlet and Sant Jaume boreholes (Ebro Delta).

Table 4. Summary of core and microfaunal data from the Carlet and Sant Jaume boreholes (Ebro Delta). Figures represent relative abundance (%) unless otherwise indicated. The single value represents the average and those in parentheses give the range.

Appendix A. Foraminiferal reference list.

Supplementary data

Table S1. Foraminiferal census data from the Carlet and Sant Jaume boreholes (Ebro Delta). The data table can be found online at the XXX website http://XXX.

Table 1. Living foraminiferal species found in and off the Ebro Delta. Above: Quantitative summary of living foraminiferal assemblages composition in different environmental settings of the modern Ebro Delta. Figures represent relative abundance (%) unless otherwise indicated. The single value represents the average and those in parentheses give the range; Below: Reference list of marine species found in the modern foraminiferal assemblages of the Ebro Delta.

Living assemblages (own data)					
***Phragmites* marsh**	***Juncus* marsh**	***Salicornia* marsh**	**Lagoon**	**Inner bay**	**Nearshore**
9 samples	7 samples	10 samples	12 samples	6 samples	2 samples
141 (65-197) standing crop ($10\ cm^3$)	150 (65-197) standing crop ($10\ cm^3$)	117 (71-201) standing crop ($10\ cm^3$)	133 (69-222) standing crop ($10\ cm^3$)	217 (197-236) standing crop ($10\ cm^3$)	196 (186-205) standing crop ($10\ cm^3$)
5 (2-9) species	6 (4-7) species	5 (2-7) species	7 (4-12) species	9 (5-14) species	23 (20-26) species
1 (0.3-0.9) Fisher alpha index	1 (0.7-1.3) Fisher alpha index	1 (0.3-1.5) Fisher alpha index	1.5 (0.7-2.4) Fisher alpha index	1.8 (0.9-3) Fisher alpha index	5.9 (4.8-7) Fisher alpha index
86.2 (48-100) agglutinated	25.6 (7-91) agglutinated	51 (0.9-100) agglutinated	1.7 (0-8.6) agglutinated	0.2 (0-1.5) agglutinated	0.8 (0.4-1.3) agglutinated
0.4 (0-2) porcellaneous	1.3 (0-5.4) porcellaneous	1.6 (0-5.2) porcellaneous	1.7 (0-12.4) porcellaneous	9.2 (0.3-17.6) porcellaneous	14.8 (12.8-16.8) porcellaneous
13.4 (0-50.1) hyaline	73.1 (9-93) hyaline	47.4 (0-99.1) hyaline	96.6 (87.4-100) hyaline	90.5 (82.4-99.7) hyaline	84.4 (82.8-86) hyaline
T. inflata 43.3 (0-88)	*T. aguayoi* 39.9 (4-79.3)	*A. beccarii* 30.8 (0-90.6)	*A. beccarii* 56 (10.8-87.4)	*A. beccarii* 68.7 (33.2-96.4)	*A. beccarii* 27.8 (19.7-36)
H. wilberti 23.3 (8.1-60.4)	*A. beccarii* 33 (2.3-86.2)	*J. macrescens* 28.3 (0-61.4)	*H. germanica* 21.7 (3.6-66.2)	*H. germanica* 12.6 (0.6-24.9)	*Q. stelligera* 12.6 (10.8-14.4)
M. fusca 11.9 (0-87.0)	*T. inflata* 18.4 (2.2-68)	*T. inflata* 22.5 (0.9-57.9)	*C. oceanensis* 9.5 (0-48.6)	*Q. jugosa* 4.4 (0-10.8)	*B. striatula* 10.1 (1.4-18.8)
T. aguayoi 10.1 (0-36)	*J. macrescens* 4.2 (0-18.4)	*H. germanica* 13.5 (0-84.6)	*C. excavatum* 4 (0-22.4)	*Q. seminula* 3.7 (0-7.5)	*B. pseudopunctata* 9.4 (5.7-13)
J. macrescens 4.9 (0-18.4)	*M. fusca* 2.3 (0-12)	*T. aguayoi* 2.9 (0-14.5)	*C. selseyense* 3 (0-14.8)	79.3 (57.3-95.5) similarity L/D	*N. opima* 8.7 (5.1-12.3)
A. beccarii 3.4 (0-29.1)	73.8 (36.4-95.5) similarity L/D	73.3 (53-94.4) similarity L/D	75.7 (52.6-91) similarity L/D		*H. depressula* 6.5 (3.5-9.5)
69.2 (31.8-87) similarity L/D					*A. mamilla* 1.3 (0.7-1.9)
					R. irregularis 0.9 (0.3-1.4)
					59.1 (57.1-61.1) similarity L/D

List of marine species (Scrutton (1969) and own data)					
Adelosina laevigata	*Cassidulina laevigata*	*Fursenkoina* cf *fusiformis*	*Massilina secans*	*Quinqueloculina longirostra*	*Textularia bocki*
Ammobaculites cf *arenaria*	*Cibicidoides bradyi*	*Fursenkoina* cf *complanata*	*Melonis pompilioides*	*Quinqueloculina rugosa*	*Textularia calva*
Ammosphaeroidina sphaeroidiniforme	*Clavulina obscura*	*Fursenkoina schreibersiana*	*Nodulina dentaliniformis*	*Quinqueloculina* sp.1	*Textularia tenuissima*
Amphicoryna scalaris	*Cornuspira incerta*	*Fursenkoina* sp.1	*Nonion asterizans*	*Rectuvigerina* cf *compressa*	*Textularia* sp.1
Asterigerinata sp.1	*Delosina complexa*	*Gaudryina* cf *rudis*	*Nonion laevigatum*	*Reophax* cf *fusiformis*	*Tretomphalus concinnus*
Aubignyina perlucida	*Eggerella advena*	*Gavelinopsis praegeri*	*Nonionella atlantica*	*Reophax cylindrica*	*Trifarina angulosa*
Brizalina cf *aenariensis*	*Elphidium advenum*	*Haplophragmoides canariensis*	*Nonionoides* cf *japonicum*	*Reophax nana*	*Triloculina dubia*
Brizalina spathulata	*Elphidium* cf *flexuosum*	*Haynesina depressula*	*Nonionoides scaphus*	*Reophax scorpiurus*	*Triloculina marioni*
Brizalina variabilis	*Elphidium* cf *schmittir*	*Hopkinsina pacifica*	*Nouria polymorphides*	*Reophax subfusiformis*	*Triloculina rotunda*
Buccella granulata	*Elphidium crispum*	*Lagena* cf *semistriata*	*Patellina corrugata*	*Reussella aculeata*	*Triloculina* sp.1
Bulimina aculeata	*Elphidium incertum*	*Lagena substriata*	*Planorbulina mediterranensis*	*Robertina arctica*	*Trochammina* cf *advena*
Bulimina elongata	*Elphidium lidoense*	*Lagena sulcata*	*Poroeponides lateralis*	*Rosalina anomala*	*Trochammina lobata*
Bulimina gibba	*Elphidium matagordanum*	*Lagena tenuis*	*Procerolagena clavata*	*Rosalina bulbosa*	*Uvigerina* sp.1
Bulimina marginata	*Elphidium* sp.1	*Lagena vulgaris*	*Psammosphaera bowmani*	*Rosalina* cf *mediterranensis*	*Valvulineria bradyana*
Bulimina sp. 1	*Elphidium* sp.2	*Lagenammina difflugiformis*	*Pyrgo inornata*	*Rosalina* cf *valvulata*	
Buliminella elegantissima	*Epistominella vitrea*	*Lagenammina laguncula*	*Quinqueloculina depressa*	*Saccammina atlantica*	
Cassidulina cf *crassa*	*Fissurina* sp.1	*Leptohalysis scottii*	*Quinqueloculina lata*	*Svratkina* sp.1	

Table 2. Dead foraminiferal species found in and off the Ebro Delta. Quantitative summary of dead foraminiferal assemblages composition in different environmental settings of the modern Ebro Delta. Figures represent relative abundance (%) unless otherwise indicated. The single value represents the average and those in parentheses give the range.

Dead assemblages (own data)					
***Phragmites* marsh**	***Juncus* marsh**	***Salicornia* marsh**	**Lagoon**	**Inner bay**	**Nearshore**
13 samples	9 samples	18 samples	18 samples	6 samples	2 samples
Water depth 0.1 (0.05-0.2) m	Water depth 0.1 (0.07-0.4) m	Water depth 0.2 (0.04-0.5) m	Water depth 0.5 (0.3-0.8) m	Water depth 0.3 (0.2-0.5) m	Water depth 7 (7-7.4) m
Sand 33 (7-66)	Sand 82 (74-94)	Sand 58 (5-81)	Sand 67 (9-92)	Sand 81 (69-92)	Sand 19 (19)
8 (5-10) species	8 (5-16) species	9 (5-15) species	7 (2-11) species	11 (8-16) species	34 (30-38) species
Fisher alpha index 1.8 (0.8-3.6)	Fisher alpha index 1.6 (0.8-3.5)	Fisher alpha index 1.9 (0.8-4.6)	Fisher alpha index 1.2 (0.3-2.1)	Fisher alpha index 2.2 (1.5-3.3)	Fisher alpha index 9 (7.4-10.7)
7 (0–50) marine tests	1 (0–7) marine tests	3 (0–13) marine tests	1 (0–6) marine tests	3 (1–6) marine tests	60 (57–62) marine tests
58 (1-99.5) agglutinated	30 (2-93) agglutinated	29 (0-94) agglutinated	0.6 (0-3) agglutinated	0.4 (0-0.9) agglutinated	4 (2-6) agglutinated
0.1 (0-0.8) porcellaneous	1 (0-5) porcellaneous	4 (0-28) porcellaneous	0.4 (0-3) porcellaneous	12 (3-22) porcellaneous	22 (22) porcellaneous
42 (0.5-99) hyaline	69 (8-98) hyaline	67 (6-99) hyaline	99 (97-100) hyaline	88 (78-97) hyaline	74 (72-77) hyaline
A. beccarii 27.1 (0-92.5)	*A. beccarii* 34.6 (2.2-84.6)	*A. beccarii* 45 (2-92.2)	*A. beccarii* 51.5 (16.9-85.7)	*A. beccarii* 77.8 (62.2-92.9)	*A. beccarii* 32.1 (26.9-37.4)
H. wilberti 23.5 (1-78.5)	*T. aguayoi* 32.8 (2.6-75.5)	*J. macrescens* 20.7 (0-70.9)	*H. germanica* 27.9 (5.3-59.3)	*Q. jugosa* 6 (0.9-12.7)	*Q. stelligera* 15.1 (14.8-15.4)
T. inflata 19.3 (0-60.1)	*T. inflata* 21.2 (0.6-70.3)	*H. germanica* 15.8 (0.3-62.8)	*C. oceanensis* 10.7 (0-32.9)	*H. germanica* 5.1 (2.8-7.4)	*H. depressula* 12.7 (11.8-13.7)
M. fusca 7.5 (0-80.8)	*J. macrescens* 4 (0-17.2)	*T. inflata* 7 (0-23.9)	*C. excavatum* 6.1 (0-28.7)	*Q. seminula* 5 (0.9-11.4)	*A. mamilla* 4.7 (3.4-6)
H. germanica 5.4 (0-36.5)	*H. wilberti* 3.8 (0-17.8)	*T. aguayoi* 3.1 (0-28.7)			*A. perlucida* 3.6 (2.5-4.8)
J. macrescens 4 (0-11.9)		*Q. seminula* 2.7 (0-20.9)			*B. pseudopunctata* 3.6 (2.5-4.8)
T. aguayoi 3.4 (0-15.8)					*Q. seminula* 3.6 (3.6)
					R. irregularis 2.8 (1.7-3.8)
Dead assemblages (Scrutton, 1969)					
Lagoon	**Lake ("Bay")**	**Transition**	**Deltaic marine**	**Inner shelf**	**Outer shelf**
2 samples	9 samples	3 samples	5 samples	15 samples	17 samples
Water depth 1 (1-1.5) m	Water depth 5.5 (2.5-9) m	Water depth 8 (6-11) m	Water depth 29 (7-51) m	Water depth 9 (3-17) m	Water depth 23 (5-50) m
Sand 37 (13-60)	Sand 23 (4-59)	Sand 12 (5-25)	Sand 4 (1-6)	Sand 59 (4-100)	Sand 15 (1-97)
3 (3-4) species	27 (16-41) species	29 (27-30) species	31 (19-40) species	32 (20-49) species	41 (22-56) species
42 (33-50) marine tests	72 (56-82) marine tests	58 (52-63) marine tests	74 (68-81) marine tests	68 (60-78) marine tests	67 (59-73) marine tests
15 (5-24) agglutinated	6 (1-13) agglutinated	9 (5-12) agglutinated	16 (3-21) agglutinated	8 (2-15) agglutinated	15 (5-24) agglutinated
20 (5-53) porcellaneous	43 (10-69) porcellaneous	29 (5-58) porcellaneous	12 (5-25) porcellaneous	42 (16-42) porcellaneous	20 (5-53) porcellaneous
65 (37-83) hyaline	51 (28-79) hyaline	62 (37-83) hyaline	72 (54-84) hyaline	50 (35-73) hyaline	65 (37-83) hyaline
A. beccarii 48 (36-60)	*A. beccarii* 21.9 (0-46)	*Q. stelligera* 10.5 (0.7-28.2)	*A. beccarii* 16.5 (0.7-64.4)	*Q. stelligera* 23.8 (1.1-62.5)	*A. beccarii* 8.5 (1.7-25.2)
H. germanica 43.5 (30.4-56.6)	*Q. stelligera* 9.7 (0-24.9)	*A. beccarii* 9.7 (6.9-11.1)	*E. scaber* 6.7 (2.7-11.5)	*A. beccarii* 15.1 (6.3-26.8)	*Q. stelligera* 6.1 (0-36.4)
	T. rotunda 5.7 (0-22.8)	*Asterigerinata* sp.1 9.1 (1.4-22)	*V. complanata* 6 (0.7-21.9)	*Asterigerinata* sp.1 8.2 (1.6-30)	*N. opima* 5.3 (0-13.3)
	E. scaber 5.4 (0-12)	*E. advenum* 8.3 (5.3-13.2)	*B. aculeata* 5.5 (0-10.8)	*N. depressulus* 5.6 (1.5-10.2)	Miliolid 13 (3.4-34)
	Miliolid 23.2 (0.8-40.2)	*Elphidium* sp.1 5.9 (1.4-11.1)	*N. opima* 5.3 (0-10.5)	*E. scaber* 5.2 (0-17.5)	
		Miliolid 15.3 (1.0-24.4)	Miliolid 8.3 (2.4-18.5)	*E. lidoense* 5.1 (0-14.4)	
				Miliolid 21.8 (13.6-38.5)	

Table 3. Radiocarbon dates from the Carlet and Sant Jaume boreholes (Ebro Delta).

Sample	Publication code	Altitude (cm)	Material	Method	Conventional C-14 age BP	$\delta^{13}C$ (‰)	Calendar calibrated age BP	2σ calibrated BP
Carlet-250	Beta-380015	-17	shells	AMS	2340±30	-8.7	2350	2360-2330
Carlet-261	Beta-380016	-28	shells	AMS	2230±30	-7.8	2305 2225 2205	2335-2150
Carlet-282	Beta-348511	-49	shells	AMS	3680±30	-9.2	4060 4050 3990	4140-4130 4090-3960 3950-3920
Carlet-284	Beta-380017	-51	shells	AMS	2130±30	-8.9	2120	2295-2270 2155-2035 2025-2005
Carlet-291	Beta-380018	-58	shells	AMS	3540±30	-7.7	3835	3895-3815 3800-3720
Carlet-307	Beta-348512	-74	shells	AMS	1560±30	-9.1	1410	1530-1380
Carlet-350	Beta-348513	-117	shells	AMS	2150±30	-9.6	2140	2300-2240 2180-2170 2160-2060
Carlet-377	Beta-380019	-144	shells	AMS	1600±30	-9.0	1525	1555-1410
Carlet-406	Beta-380020	-173	shells	AMS	1630±30	-8.6	1535	1570-1515 1490-1485 1460-1415
Carlet-416	Beta-348514	-183	shells	AMS	1700±30	-8.5	1600 1580 1570	1700-1540
Carlet-423	Beta-348515	-190	shells	AMS	1770±30	-8.4	1700	1770-1760 1740-1610
Carlet-440	Beta-380021	-207	shells	AMS	2540±30	-7.3	2720	2745-2695 2635-2615 2595-2500
Carlet-448	Beta-348516	-215	shells	AMS	2490±30	-7.5	2700 2640 2620 2590 2540 2530 2520	2720-2460
Carlet-611	Beta-348517	-378	wood	AMS	2000±30	-25.5	1950	2000-1880
Carlet-1251	Beta-380023	-1018	shells	AMS	370±30	-9.4	465	505-420 405-315
Carlet-1256	Beta-348518	-1023	wood	AMS	06.3±0.3 pMC*	-26.1	-	-
Carlet-1261	Beta-380024	-1028	shells	AMS	2670±30	-8.3	2765	2840-2825 2795-2750
Carlet-1274	Beta-354495	-1041	wood	AMS	2980±30	-26.5	3200 3190 3160	3260-3070
Carlet-1368	Beta-380025	-1135	shells	AMS	4032±42**	-2.5	4065	4155-3930
Carlet-1405	Beta-380026	-1172	shells	AMS	4252±42**	-0.7	4385	4445-4240
Carlet-1411	Beta-380027	-1178	shells	AMS	4062±42**	+0.2	4085	4220-3970
Carlet-1435	Beta-380028	-1202	shells	AMS	4162±42**	NA	4230	4375-4125
Carlet-1596	Beta-380030	-1363	shells	AMS	6262±50**	NA	6715	6835-6615
Carlet-1706	Beta-354496	-1473	shells	AMS	7270±50**	-1.6	7720	7830-7630
Carlet-1731	Beta-354497	-1498	shells	AMS	1710±40**	+2.1	1260	1320-1200
Carlet-1741	Beta-380031	-1508	shells	AMS	7432±42**	-1.4	7915	7965-7815

Carlet-1751	Beta-380032	-1518	shells	AMS	7402±42**	-1.3	7865	7945-7785
Carlet-1798	Beta-380033	-1565	shells	AMS	7422±50**	+1.3	7905	7970-7785
Carlet-1843	Beta-380034	-1610	shells	AMS	7502±42**	-4.0	7955	8020-7900
Carlet-1910	OS-90972	-1677	shells	AMS	7620±35**	-2.82	7955	8043-7866
StJaume-528	Beta-354498	-426	shells	AMS	560±40**	-0.7	240	280-80 post-1950 CE
StJaume-626	Beta-354499	-524	shells	AMS	680±40**	-2.6	300	420-260
StJaume-651	Beta-354500	-549	shells	AMS	870±40**	-2.7	490	530-440
StJaume-1128	Beta-373725	-1026	shells	AMS	890±40**	+0.4	500	545-460
StJaume-1261	Beta-373726	-1159	shells	AMS	1120±40**	0.0	665	730-630
StJaume-1517	Beta-373727	-1415	shells	AMS	1250±40**	+2.8	780	895-700
StJaume-1527	Beta-373728	-1425	shells	AMS	1360±40**	+0.9	910	970-820
StJaume-1584	Beta-373729	-1482	shells	AMS	1310±40**	-3.0	880	925-765
StJaume-1654	Beta-373730	-1552	shells	AMS	1870±40**	+0.6	1400	1515-1325
StJaume-1847	Beta-373731	-1745	shells	AMS	1240±40**	+1.8	775	890-690
StJaume-1853	Beta-354501	-1751	shells	AMS	1730±40**	+2.9	1280	1340-1220
StJaume-1949	Beta-373732	-1847	shells	AMS	1760±40**	+0.3	1295	1370-1255

* pMC: percent modern carbon; the material was living about the last 60 years or so.
** adjusted for marine reservoir with a local deltaR correction of 120 years.
NA: sample too small to provide a 13C/12C ratio on the original material.

Table 4. Summary of core and microfaunal data from the Carlet and Sant Jaume boreholes (Ebro Delta). Figures represent relative abundance (%) unless otherwise indicated. The single value represents the average and those in parentheses give the range.

Carlet	Sant Jaume
DI 1	DI 1
Elevational range +1.44-1.29 m	Elevational range 0.73-4.04 m
Thickness 2.73 m	Thickness 3.31 m
Sand 9 (0.9-16.8)	Sand 17.3 (0.1-98.2)
Radiocarbon age 1560±30, 2130±30, 2150±30, 2230±30, 2340±30, 3540±30, 3680±30 BP	Age < 500 BP
Few tests of *A. beccarii*	Few foraminifera
Terrestrial gastropods	
Oogonia of Characeae algae	
DI 2	DI 2
Elevational range 1.29-2.27 m	Elevational range 4.04-8.16 m
Thickness 0.98 m	Thickness 4.12 m
Sand 3 (0.4-10.6)	Sand 1 (0.1-5.3)
Radiocarbon age 1600±30, 1630±30, 1700±30, 1770±30, 2490±30, 2540±30 BP	Radiocarbon age 560±40, 680±40, 870±40 BP
Very abundant tests	Very abundant tests
1 (1-2) species	14 (6-28) species
Fisher alpha index 0.2 (0.1-0.3)	Fisher alpha index 3 (1.2-6.8)
0 (0-0) marine tests	15 (0.6-52.5) marine tests
0 (0-0) agglutinated	0.1 (0-0.9) agglutinated
0 (0-0) porcellaneous	5 (0.5-20.9) porcellaneous
100 (100-100) hyaline	95 (78.7-99.5) hyaline
A. beccarii 99 (94.9-100)	*A. beccarii* 52 (27.3-67.7)
Terrestrial gastropods	*H. germanica* 11 (0.4-40)
Oogonia of Characeae algae	*C. oceanensis* 11 (0-48.1)
	C. selseyense 8 (0-21)
	B. variabilis 6 (0-20.7)
DI 3	DI 3
Elevational range 2.27-5.94 m	Elevational range 8.16-11.56 m
Thickness 3.67 m	Thickness 3.4 m
Sand 67 (28.1-98.2)	Sand 10 (0.1-80.1)
Radiocarbon age 2000±30 BP	Radiocarbon age 890±40 BP
Few foraminifera	Irregular abundance of tests
	18 (10-28) species
	Fisher alpha index 4.6 (1.4-7.9)
	34 (3.8-60.1) marine tests
	0.5 (0-2.3) agglutinated
	16 (1.2-32.6) porcellaneous
	84 (65.1-98.8) hyaline
	A. beccarii 38 (11.6-74.9)
	C. selseyense 18 (3.1-72.4)
	A. mamilla 11 (0-36.7)
	Q. oblonga 3 (0-11.9)
	Q. seminula 3 (0-10.7)
	H. germanica 3 (0.4-7.8)

DI 4
Elevational range 5.94-9.48 m
Thickness 3.54 m
Sand 86 (47.7-95.6)
Irregular abundance of tests
21 (17-24) species
Fisher alpha index 6.1 (5.6-7.7)
34 (32-37.1) marine tests
0.7 (0-1.4) agglutinated
35 (18.7-41.6) porcellaneous
65 (58-79.9) hyaline
A. beccarii 36 (31.5-41.5)
Q. seminula 18 (9.5-21.1)
C. selseyense 13 (10-16)
R. anomala 6 (1.6-9.2)
T. marioni 6 (2-11.9)
C. lobatulus 4 (3.1-5.6)

DI 5
Elevational range 9.48-16.94 m
Thickness 7.54 m
Sand 7 (0.4-52.2)
Radiocarbon age 370±30, 1710±40, 2670±30, 2980±30, 4032±42, 4062±42, 4162±42, 4252±42, 6262±50, 7270±50, 7402±42, 7422±50, 7432±42, 7502±42, 7620±35 BP
Irregular abundance in the upper 2.7 m
10 (4-17) species
Fisher alpha index 2.4 (0.8-5.8)
7 (0.3-37.5) marine tests
0.1 (0-1.2) agglutinated
8 (0-36.5) porcellaneous
92 (63.5-100) hyaline
A. beccarii 74 (29.9-97.3)
C. selseyense 13 (0.3-35.4)
Q. seminula 4 (0-14.6)

DI 4
Elevational range 11.56-17.81 m
Thickness 6.25 m
Sand 1 (0.3-2.5)
Radiocarbon age 1120±40, 1240±40, 1250±40, 1310±40, 1360±40, 1730±40 1870±40 BP
Irregular abundance in the upper 2.7 m
13 (4-22) species
Fisher alpha index 3.3 (1-5.8)
8 (0-17.7) marine tests
0.3 (0-1.8) agglutinated
5 (1-10.7) porcellaneous
95 (89.3-99) hyaline
A. beccarii 65 (40.2-92.4)
C. selseyense 19 (2.3-35.9)
Q. seminula 3 (0-9.2)
C. poeyanum 3 (0-7.7)

DI 5
Elevational range 17.81-20.93 m
Thickness 3.12 m
Sand 5 (0.2-19.1)
Radiocarbon age 1760±40 BP
Irregular abundance of tests
22 (10-35) species
Fisher alpha index 7.6 (2.4-12.4)
43 (26.5-69.5) marine tests
1 (0-6.5) agglutinated
24 (3.4-38.9) porcellaneous
75 (61.1-96.6) hyaline
C. selseyense 18 (0-47.4)
A. beccarii 13 (4.5-22.2)
Q. seminula 11 (2-25.2)
C. poeyanum 6 (0-22.1)
B. variabilis 5 (0-13.4)
B. gibba 4 (0-10.7)
V. bradyana 3 (0-17.3)
R. irregularis 3 (0-13.4)

Appendix A. Foraminiferal reference list.

Agglutinated forms

Eggerelloides scaber (Williamson) = *Bulimina scabra* Williamson, 1858

Haplophragmoides wilberti Anderson, 1953

Jadammina macrescens (Brady) = *Trochammina inflata* (Montagu) var. *macrescens* Brady, 1870

Textularia agglutinans d'Orbigny, 1839

Textularia bocki Höglund, 1947

Textularia calva Lalicker, 1935

Textularia sp.

Trochammina inflata (Montagu) = *Nautilus inflatus* Montagu, 1808

Porcellaneous forms

Adelosina bicornis (Walker and Jacob) = *Serpula bicornis* Walker and Jacob, 1798

Adelosina laevigata (d'Orbigny) = *Quinqueloculina laevigata* d'Orbigny, 1939

Adelosina mediterranensis (Le Calvez and Le Calvez) = *Quinqueloculina mediterranensis* Le Calvez and Le Calvez, 1958

Adelosina striata d'Orbigny, 1826

Adelosina sp.

Cornuloculina sp.

Cornuspira incerta (d'Orbigny) = *Operculina incerta* d'Orbigny, 1839

Cornuspira involvens (Reuss) = *Operculina involvens* Reus, 1850

Lachlanella undulata (d'Orbigny) = *Quinqueloculina undulata* d'Orbigny, 1852

Massilina secans (d'Orbigny) = *Quinqueloculina secans* d'Orbigny, 1826

Miliolinella subrotunda (Montagu) = *Vermiculum subrotundum* Montagu, 1803

Miliolinella webbiana (d'Orbigny) = *Triloculina webbiana* d'Orbigny, 1839

Pyrgo inornata (d'Orbigny) = *Biloculina inornata* d'Orbigny, 1846

Pyrgo sp.

Quinqueloculina berthelotiana d'Orbigny, 1839

Quinqueloculina depressa d'Orbigny, 1852

Quinqueloculina lata Terquem, 1876

Quinqueloculina longirostra d'Orbigny, 1826

Quinqueloculina oblonga (Montagu) = *Vermiculum oblongum* Montagu, 1893

Quinqueloculina seminula (Linné) = *Serpula seminulum* Linné, 1758

Quinqueloculina stelligera Schlumberger, 1893

Quinqueloculina vulgaris d'Orbigny, 1826

Quinqueloculina sp.1

Quinqueloculina sp.2

Siphonaperta quadrata (Nørvang) = *Quinqueloculina quadrata* Nørvang, 1945

Triloculina dubia d'Orbigny, 1826

Triloculina marioni Schlumberger, 1893

Triloculina rotunda d'Orbigny, 1939

Triloculina trigonula (Lamarck) = *Miliolites trigonula* Lamarck, 1804

Hyaline forms

Acervulina inhaerens Schulze, 1854

Ammonia beccarii (Linné) = *Nautilus beccarii* Linné, 1758 (Variants included in this taxon)

Astacolus crepidulus (Fichtel and Moll) = *Nautilus crepidula* Fichtel and Moll, 1798

Asterigerinata mamilla (Williamson) = *Rotalia mamilla* Williamson, 1858

Aubignyna hamblensis Murray, Whittaker and Alve, 2000

Aubignyna perlucida (Heron-Allen and Earland) = *Rotalia perlucida* Heron-Allen and Earland, 1913

Bolivina difformis (Williamson) = *Textularia variabilis* var. *difformis* Williamson, 1858

Bolivina dilatata Reuss, 1850

Bolivina pseudoplicata Heron-Allen and Earland, 1930

Bolivina striatula (Cushman) = *Brizalina striatula* Cushman, 1922

Bolivinellina pseudopunctata (Höglund) = *Bolivina pseudopunctata* Höglund, 1947

Brizalina spathulata (Williamson) = *Textularia variabilis* Williamson var. *spathulata* Williamson, 1858

Brizalina variabilis (Williamson) = *Textularia variabilis* Williamson, 1859

Buccella granulata (di Napoli Alliata) = *Eponides frigidus* var. *granulatus* di Napoli Alliata, 1952

Bulimina aculeata d'Orbigny, 1926

Bulimina elongata d'Orbigny, 1926

Bulimina gibba Fornasini, 1902

Bulimina marginata d'Orbigny, 1826

Buliminella elegantissima (d'Orbigny) = *Bulimina elegantissima* d'Orbigny, 1939

Cassidulina carinata Silvestri, 1896

Cassidulina obtusa Williamson, 1858

Cibicides lobatulus (Walker and Jacob) = *Nautilus lobatulus* Walker and Jacob, 1798

Cibicides sp.

Cribroelphidium excavatum (Terquem) = *Polystomella excavatum* Terquem, 1875

Cribroelphidium magellanicum (Heron-Allen and Earland) = *Elphidium magellanicum* Heron-Allen and Earland, 1932

Cribroelphidium oceanensis (d'Orbigny) = *Polystomella oceanensis* d'Orbigny, 1826

Cribroelphidium poeyanum (d'Orbigny, 1826) = *Polystomella poeyana* d'Orbigny, 1826

Cribroelphidium selseyense (Heron-Allen and Earland) = *Elphidium selseyensis* Heron-Allen and Earland, 1911

Cribroelphidium williamsoni (Haynes) = *Elphidium williamsoni* Haynes, 1973

Discorbis sp.

Elphidium advenum (Cushman) = *Polystomella advenum* Cushman, 1922

Elphidium crispum (Linné) = *Nautilis crispus* Linné, 1758

Elphidium erlandi Cushman, 1936

Elphidium flexuosum (d'Orbigny) = *Polystomella flexuosa* d'Orbigny, 1936

Elphidium gerthi Van Voorthuysen, 1957

Elphidium incertum (Williamson) = *Polystomella umbilicatula* var. *incerta* Williamson, 1858

Elphidium macellum (Fichtel and Moll) = *Nautilus macellus* Fichtel and Moll, 1798

Elphidium margaritaceum Cushman, 1930

Elphidium sp.

Epistominella vitrea Parker, 1953

Favulina melo (d'Orbigny) = *Oolina melo* d'Orbigny, 1839

Fissurina lucida (Williamson) = *Entosolenia marginata* (Montagu) var. *lucida* Williamson, 1848

Fissurina marginata (Montagu) = *Vermiculum marginatum* Montagu, 1803

Fissurina sp.

Fursenkoina schreibersiana (Czjzek) = *Virgulina schreibersiana* Czjzek, 1848

Gavelinopsis praegeri (Heron-Allen and Earland) = *Discorbina praegeri* Heron-Allen and Earland, 1913

Globobulimina sp.

Gyroidina sp.

Haynesina depressula (Water and Jacob) = *Nautilus depressulus* Walker and Jacob, 1798

Haynesina germanica (Ehrenberg) = *Nonionina germanica* Ehrenberg, 1840

Lagena semistriata (Williamson) = *Lagena striata* Walker var. *semistriata* Williamson, 1848

Lagena sulcata (Walter and Jacob) = *Serpula sulcata* Walter and Jacob, 1798

Lagena vulgaris Williamson, 1858

Nonionella atlantica Cushman, 1947

Nonionella opima Cushman, 1947

Nonionoides boueanum (d'Orbigny) = *Nonionina boueana* d'Orbigny, 1846

Nonionoides turgida (Williamson) = *Nonionina turgida* Williamson, 1858

Patellina corrugata Williamson, 1858

Planorbulina mediterranensis d'Orbigny, 1826

Rectuvigerina compressa (Cushman) = *Uvigerina compressa* Cushman, 1925

Reussella aculeata Cushman, 1945

Reussoolina laevis (Montagu) = *Vermiculum laeve* Montagu, 1803

Rosalina anomala Terquem, 1875

Rosalina globularis d'Orbigny, 1826

Rosalina irregularis (Rhumbler) = *Discorbina irregularis* Rhumbler, 1906

Rosalina valvulata d'Orbigny, 1826

Rosalina williamsoni (Chapman and Parr) = *Discorbis williamsoni* Chapman and Parr, 1932

Rosalina sp. 1

Rosalina sp. 2

Spirillina vivipara Ehrenberg, 1843

Svratkina sp.

Tretomphaloides concinnus (Brady) = *Discorbina concinna* Brady, 1884

Trichohyalus aguayoi (Bermudez) = *Discorinopsis aguayoi* Bermudez, 1935

Trifarina angulosa (Williamson) = *Uvigerina angulosa* Williamson, 1858

Uvigerina peregrina Cushman, 1923

Valvulineria bradyana (Fornasini) = *Discorbina bradyana* Fornasini, 1899

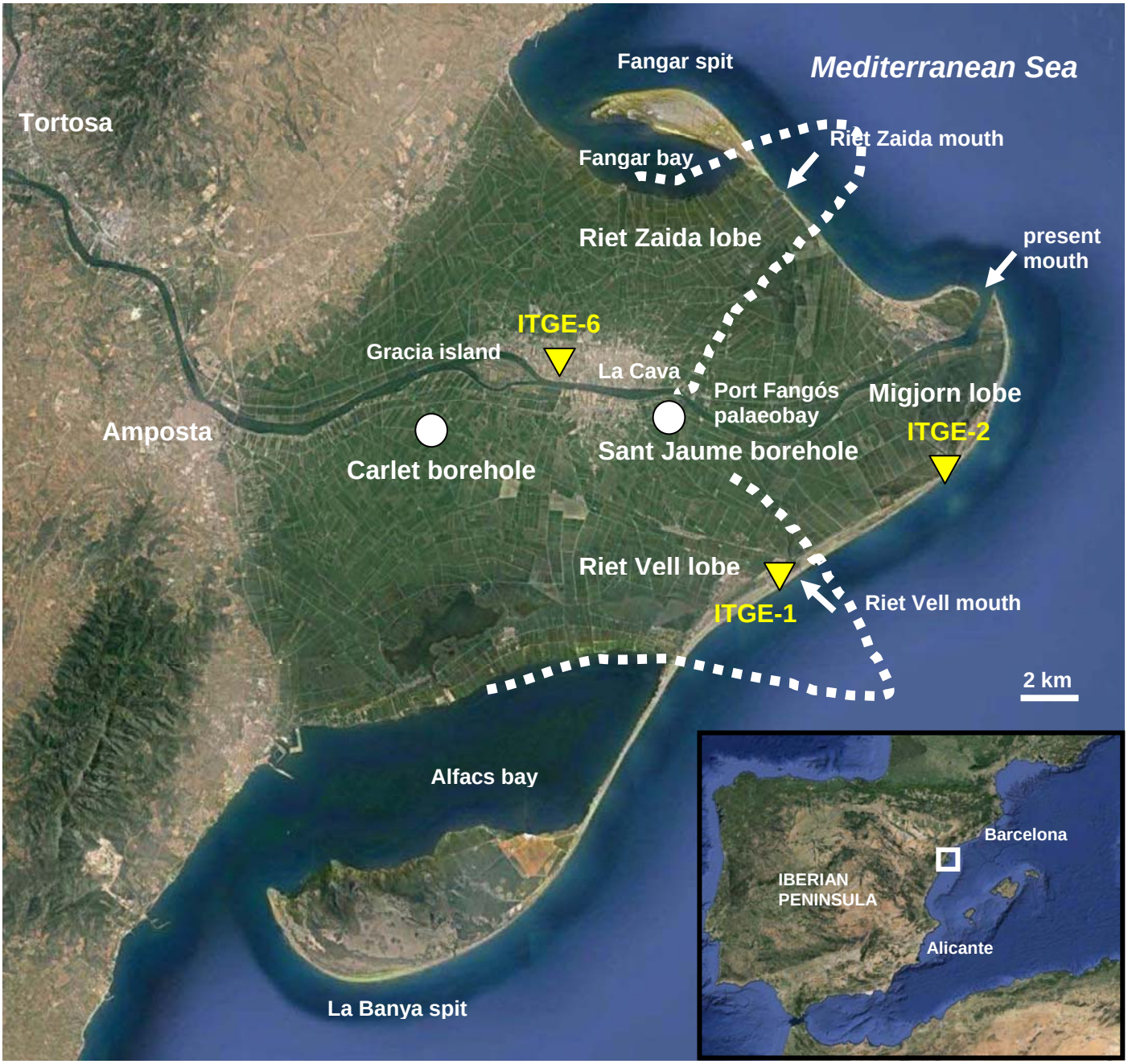
Fangar spit
Mediterranean Sea
Tortosa
Riet Zaida mouth
Fangar bay
Riet Zaida lobe
present mouth
ITGE-6
Gracia island
La Cava
Port Fangós palaeobay
Migjorn lobe
Amposta
ITGE-2
Carlet borehole
Sant Jaume borehole
Riet Vell lobe
ITGE-1
Riet Vell mouth
2 km
Alfacs bay
Barcelona
IBERIAN PENINSULA
Alicante
La Banya spit

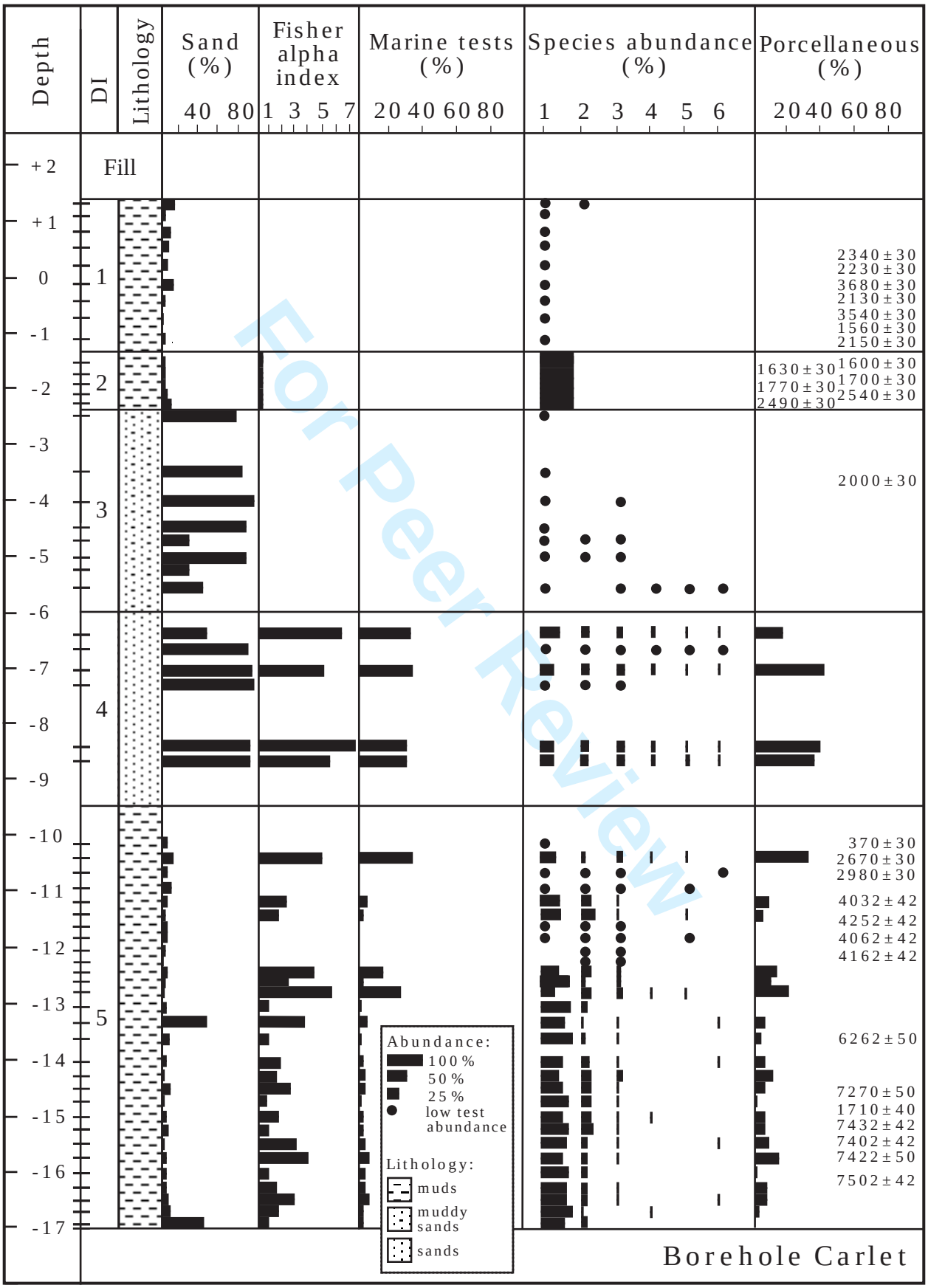

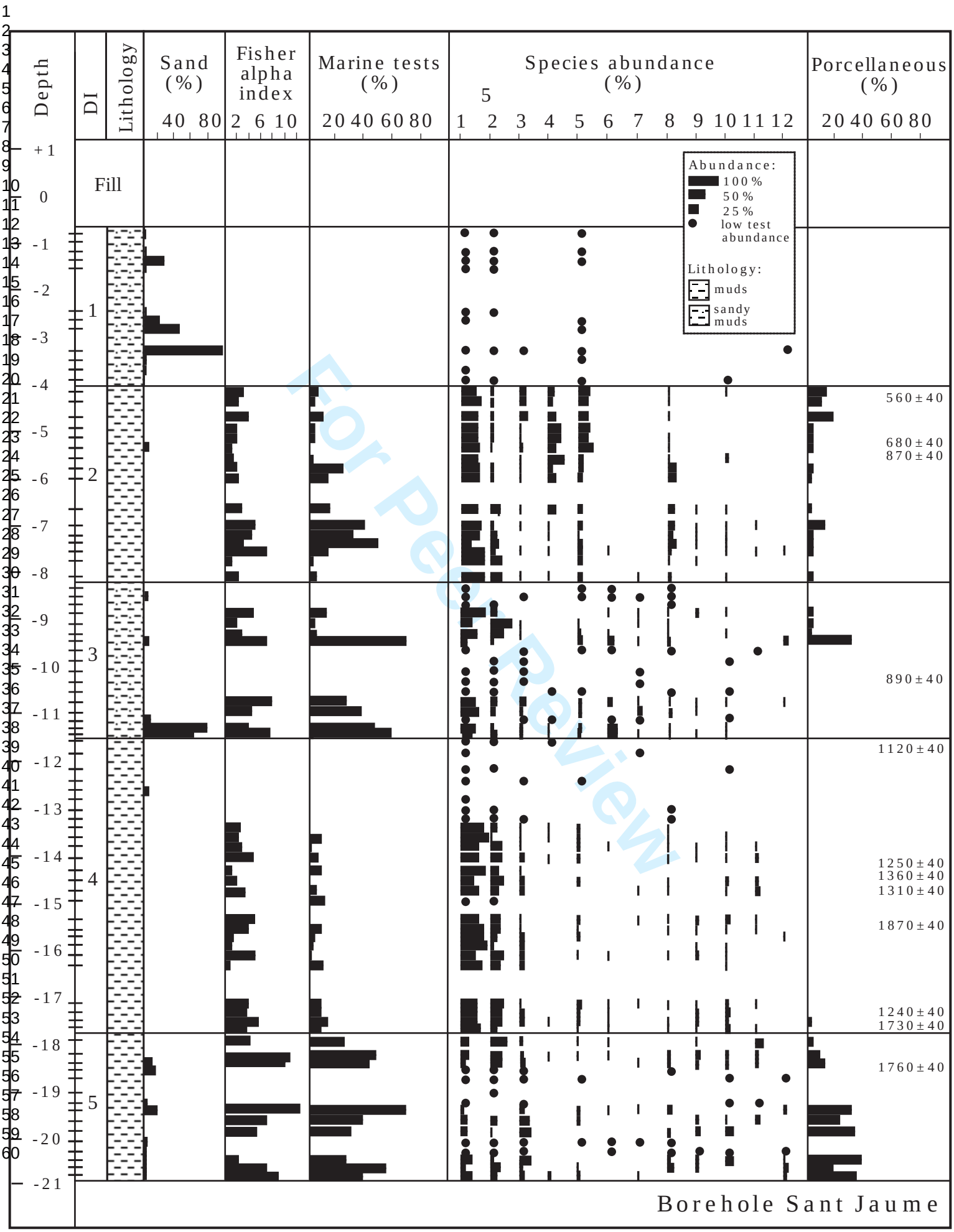

Carlet

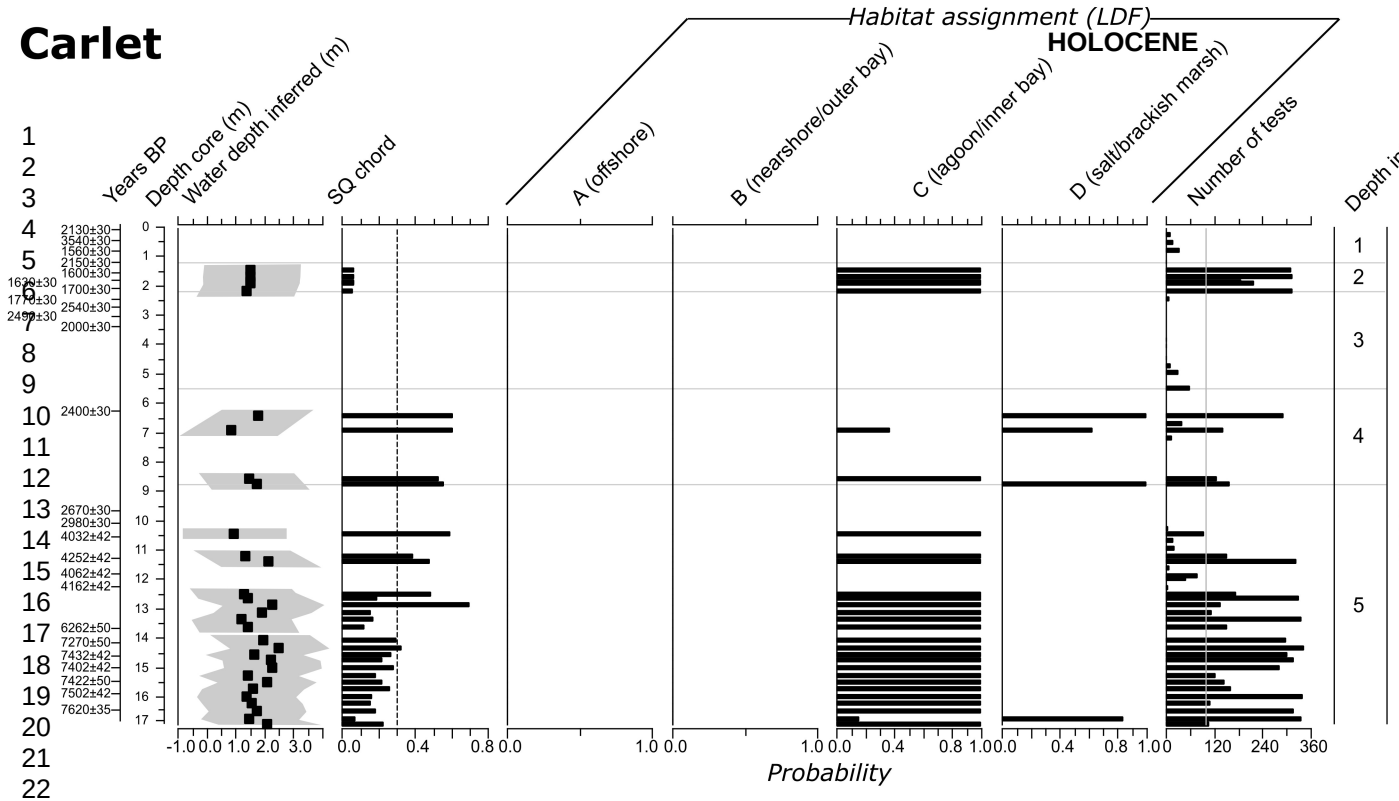

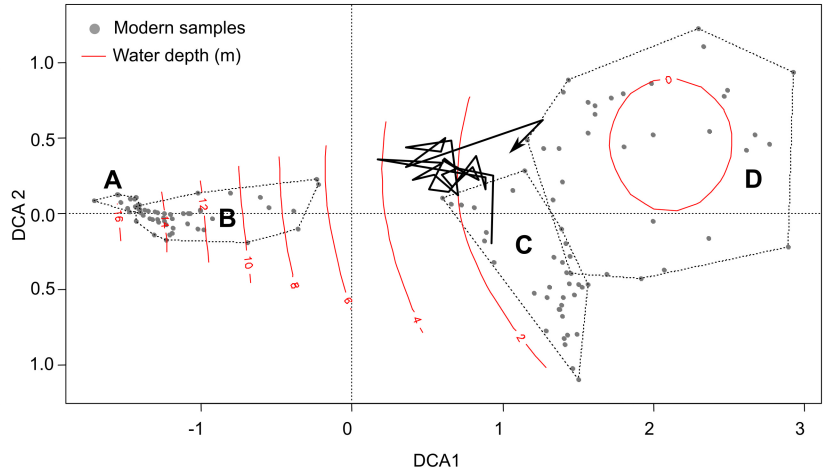

Sant Jaume

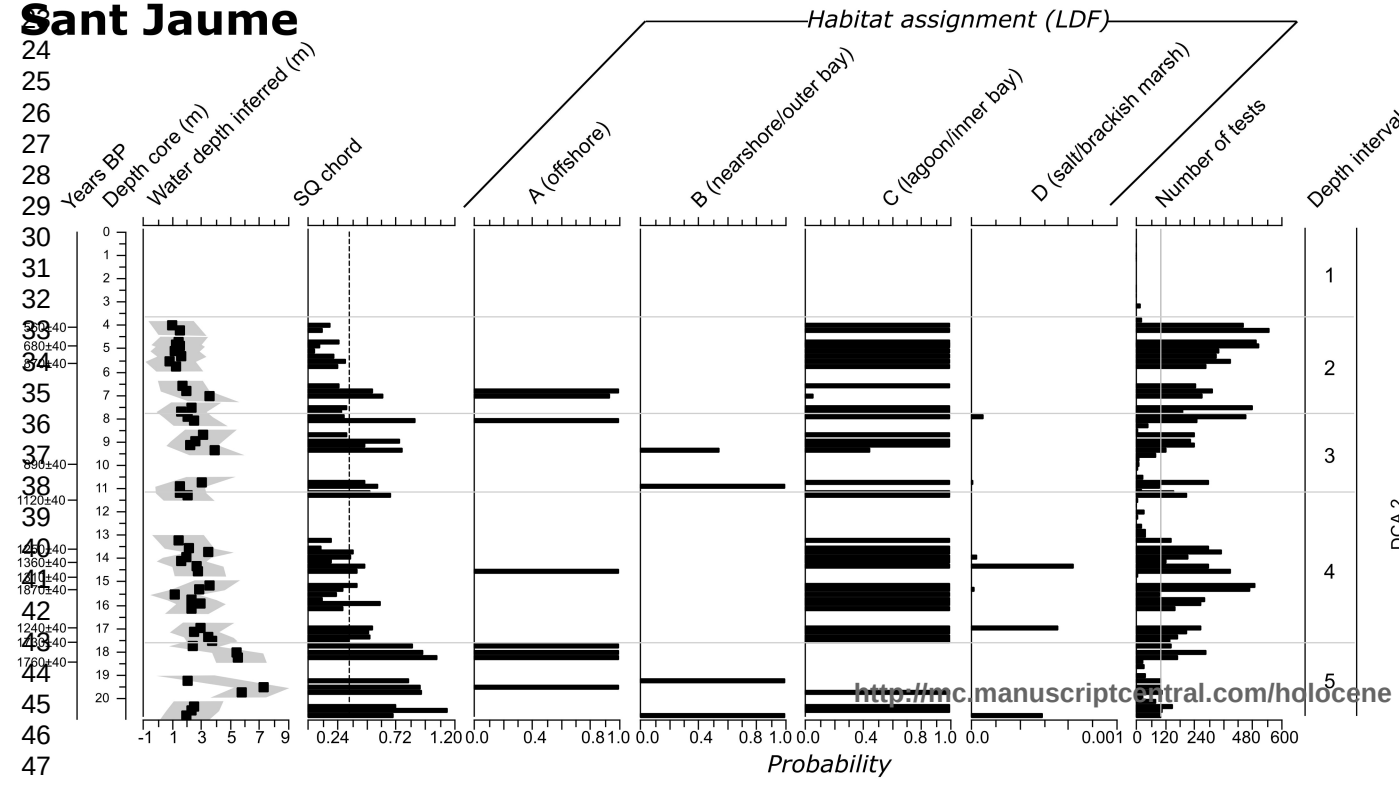

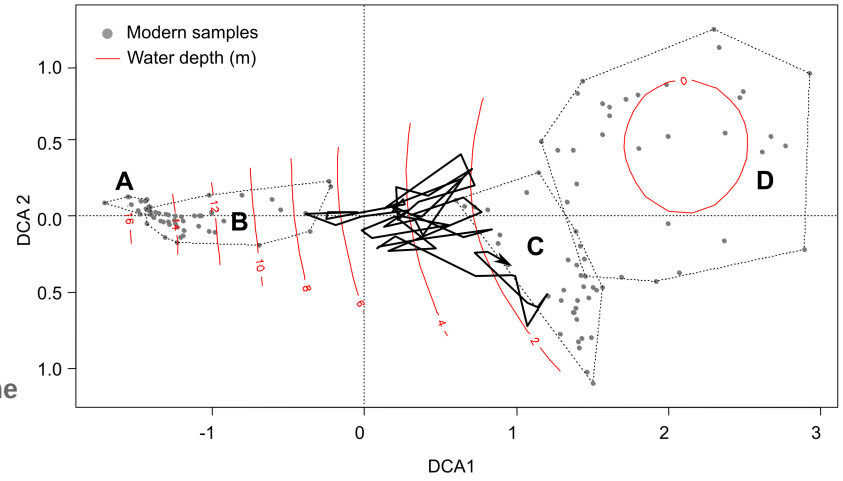

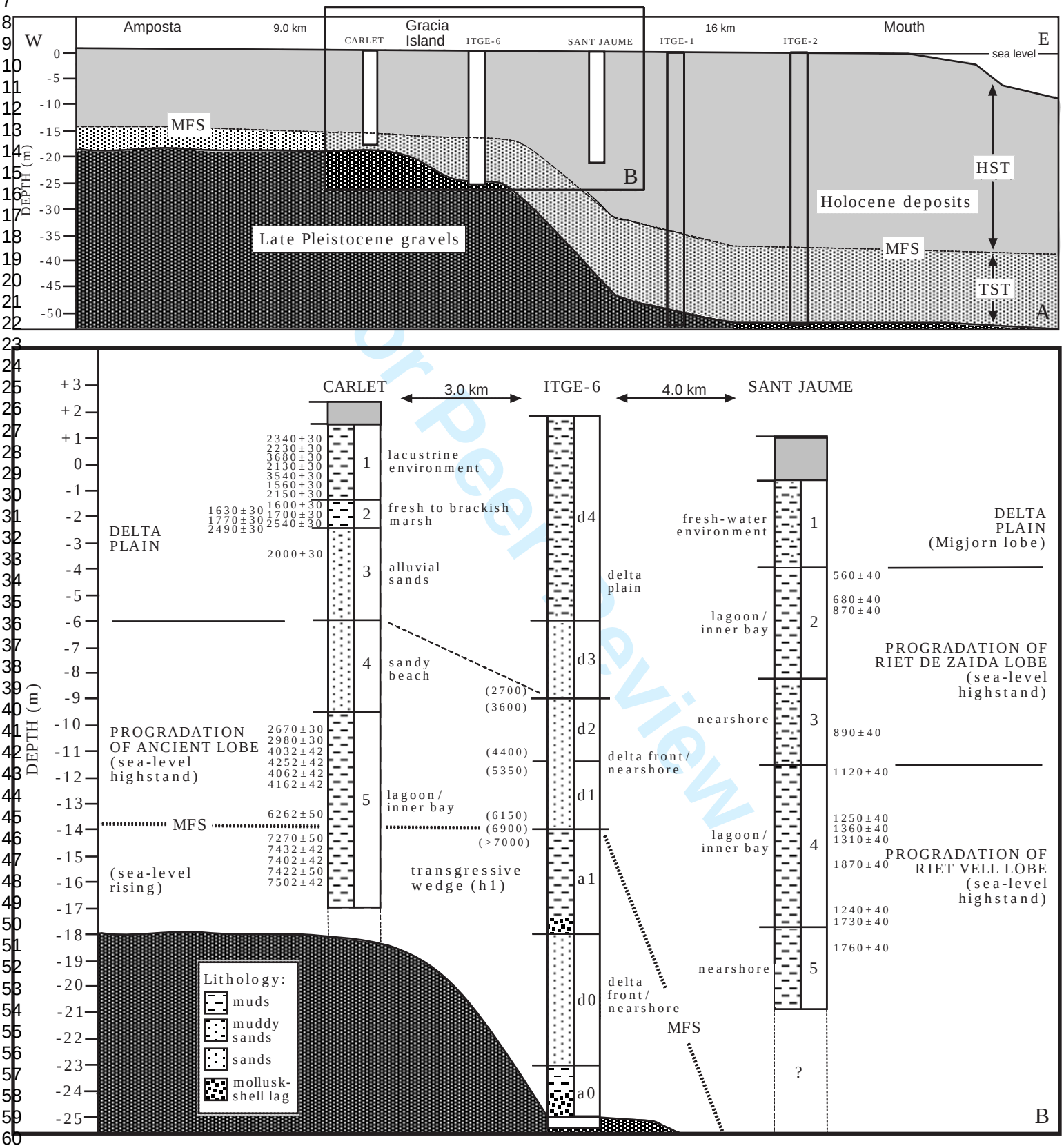

Carlet borehole (Ebro Delta)

Sample	Depth (cm)	*Textularia bocki*	*Trochammina inflata*	*Adelosina bicornis*	*Adelosina laevigata*	*Adelosina striata*	*Cornuspira involvens*	*Massilina secans*	*Miliolinella subrotunda*	*Miliolinella webbiana*	*Quinqueloculina bertheliotiana*	*Quinqueloculina lata*	*Quinqueloculina oblonga*	*Quinqueloculina seminula*	*Siphonaperta quadrata*	*Triloculina marioni*	*Triloculina trigonula*	*Ammonia beccarii*	*Asterigerinata mamilla*	*Aubignyna hamblensis*	*Bolivina pseudoplicata*	*Brizalina variabilis*	*Bulimina elongata*	*Bulimina gibba*	*Cassidulina carinata*	*Cibicides lobatulus*	*Cribroelphidium excavatum*	*Cribroelphidium oceanensis*	*Cribroelphidium selseyense*	*Discorbis* sp.	*Elphidium crispum*	*Elphidium margaritaceum*	*Fissurina lucida*
1	134		*															*											*				
2	109																	*															
3	84																	*															
4	31																	*															
5	1																	*															
6	-24																	*															
7	-49																	*															
8	-74																	*															
9	-117																	*															
10	-142																	100															
11	-167																	100															
12	-183																	100															
13	-190																	100															
14	-215																	94.9															
15	-240				*													*									*						
16	-378																	*															
17	-402													*				*															
18	-444																	*															
19	-469													*				*		*								*	*		*			
20	-494	*												*			*	*									*	*	*	*				
21	-519																																	
22	-544				*									*	*	*		*								*	*						
23	-640	1.4			2.0			1.4				0.7		9.5		2.0	3.1	41.5	0.3	1.0	0.7	1.4	0.3	1.7		5.1	1.7		16.0		1.0	0.3	
24	-665	*			*			*				*		*		*	*	*								*			*				
25	-690	0.7			6.3	0.7		2.8		0.7		2.8		19.6		5.6	2.8	31.5		0.7						5.6			10.5			0.7	
26	-715				*									*			*	*					*						*			*	

27	-854	0.8			1.6			1.6		0.8		3.9		21.1	0.8	3.9	7.0	33.6		0.8			0.8	0.8		3.9	1.6		14.8					
28	-873				1.9	1.3		1.3					0.6	20.6		11.9		35.6	0.6	0.6			1.3			3.1			10.0	0.6	0.6	0.6		
29	-1023																	*																
30	-1041			1.0	1.0	3.1	1.0		1.0					14.6		2.1	12.5	45.8										1.0	7.3			1.0		
31	-1066						*							*				*								*			*					
32	-1091												*	*		*		*						*					*	*				
33	-1116				3.9	0.6			0.6					2.6				61.0			0.6		0.6				2.6		24.0	0.6				
34	-1135				1.2									1.2		0.6	0.3	59.7					0.3						35.4	0.3	0.9			
35	-1160	*												*				*											*					
36	-1185	*			*									*		*		*				*	*	*					*	*				
37	-1198													*						*							*		*		*			
38	-1223													*															*					
39	-1247			0.6	0.3				3.4				1.7	8.0				47.4						0.3			1.7		24.6		1.7	1.1		
40	-1259				0.6		0.6		0.3				0.6	6.9				82.2	0.3			0.6	0.3		0.3				6.9					
41	-1284						1.5					0.7	1.5	13.1		3.6	2.2	29.9		6.7		2.2	7.3	2.9					22.6		0.7		0.7	
42	-1309																	88.8					0.7				0.7		8.6					
43	-1334						0.3		0.6				0.9	2.7			0.9	79.5			0.6		0.3	0.3		0.6	4.2		1.2			1.5		
44	-1359								0.7					1.3				92.2		0.7									5.2					
45	-1405				0.3								0.3	3.7			1.0	73.7		0.3						0.3	3.0		16.7		2.0			
46	-1430	1.2					0.3							12.2				59.1		0.6			0.9				4.3		18.0		3.5			
47	-1455				1.0	0.3	0.3					0.3		2.0			1.3	75.6		2.0		0.3							14.2		0.7			
48	-1473													0.9				82.8		0.3									15.7		0.3			
49	-1498													3.5			0.7	73.6		0.4			0.4						20.0		0.4			
50	-1523												0.8	4.0				84.0				0.8							10.4					
51	-1548				0.7		0.7							6.2			0.7	77.9	0.7	0.7						0.7	1.4		9.0		0.7			
52	-1570			0.6		0.6	1.9						1.9	7.5	0.6			71.4	0.6	0.6		1.2	0.6				1.9		8.1					
53	-1595				0.3								0.6					89.1	0.3										8.8					
54	-1620							0.9			0.9			2.7				85.8									1.8		8.0					
55	-1645	0.9			0.9									1.6			2.2	84.0					0.6		0.3	0.3	0.9		6.6					
56	-1670						0.3						0.6				0.3	97.3									0.3	0.3	0.3					
57	-1690																	78.0									10.1		9.2		1.8			

Fissurina marginata	*Gavelinopsis praegeri*	*Gyroidina* sp.	*Haynesina depressula*	*Haynesina germanica*	*Nonionella atlantica*	*Nonionoides boueanum*	*Planorbulina mediterranensis*	*Rosalina irregularis*	*Rosalina anomala*	*Spirillina vivipara*	*Trichohyalus aguayoi*	Number of foraminifera studied	Number of species	Fisher alpha index	Agglutinated tests %	Porcellaneous tests %	Hyaline tests %	Marine tests %
												9	3	-	-	-	-	-
												4	1	-	-	-	-	-
												44	1	-	-	-	-	-
												5	1	-	-	-	-	-
											*	2	2	-	-	-	-	-
											*	12	2	-	-	-	-	-
												19	1	-	-	-	-	-
											*	36	2	-	-	-	-	-
												2	1	-	-	-	-	-
												313	1	0.13	0.0	0.0	100	0.0
												316	1	0.13	0.0	0.0	100	0.0
												189	1	0.14	0.0	0.0	100	0.0
												220	1	0.14	0.0	0.0	100	0.0
											5.1	316	2	0.29	0.0	0.0	100	0.0
												9	3	-	-	-	-	-
												2	1	-	-	-	-	-
												4	2	-	-	-	-	-
												3	1	-	-	-	-	-
												12	6	-	-	-	-	-
											*	31	9	-	-	-	-	-
												0	0	-	-	-	-	-
				*			*	*	*			60	10	-	-	-	-	-
			1.4			0.3	1.7	3.1	9.2			294	24	6.18	1.4	18.7	79.9	36.1
								*	*			40	12	-	-	-	-	-
				1.4				3.5	4.9			143	17	5.03	0.7	41.3	58.0	37.1
								*				16	8	-	-	-	-	-

		0.8		0.8			2.3	0.8	1.6		0.8	128	22	7.65	0.8	40.6	59.4	32.0
			0.6	0.6			1.3		6.9			160	19	5.61	0.0	37.5	62.5	32.5
												6	1	-	-	-	-	-
								12.5	1.0	2.1		96	15	4.99	0.0	36.5	63.5	37.5
												19	5	-	-	-	-	-
											*	21	8	-	-	-	-	-
												154	10	2.39	0.0	7.7	92.3	6.3
												325	9	1.71	0.0	3.4	96.6	3.7
												8	4	-	-	-	-	-
												80	10	-	-	-	-	-
												52	5	-	-	-	-	-
												5	2	-	-	-	-	-
	1.1		0.3			0.6		4.6		1.7		175	16	4.29	0.0	14.3	85.7	18.3
										0.3		331	12	2.44	0.0	9.1	90.9	3.3
			1.5		2.2				1.5			137	17	5.77	0.0	22.6	77.4	26.3
								0.7				116	5	1.06	0.0	0.0	100	1.4
				3.3				2.7		0.3	0.6	337	17	3.78	0.0	5.3	94.7	8.0
												153	5	0.99	0.0	2.0	98.0	0.7
												300	10	1.99	0.0	5.3	94.7	3.9
												345	9	1.69	1.2	12.5	86.3	5.5
	0.3							1.7				303	13	2.76	0.0	5.3	94.7	5.9
												319	5	0.84	0.0	0.9	99.1	0.3
0.4									0.4			284	9	1.77	0.0	4.2	95.8	2.1
												125	5	1.04	0.0	4.8	95.2	1.6
								0.7				145	11	3.10	0.0	8.3	91.7	4.1
				0.6				1.9				161	15	4.04	0.0	13.0	87.0	8.1
								0.9				341	6	1.03	0.0	0.9	99.1	2.1
								0.9				113	7	1.65	0.0	4.5	95.5	2.7
	0.3		0.6			0.3		0.3				318	14	2.99	0.9	4.7	94.4	6.3
			0.3						0.3			337	9	1.70	0.0	1.5	98.5	1.3
				0.9								109	5	1.08	0.0	0.0	100	1.8
												7604	**44**					

Sant Jaume borehole (Ebro Delta)

Sample	Depth (cm)	*Eggerelloides scaber*	*Haplophragmoides wilberti*	*Jadammina macrescens*	*Textularia agglutinans*	*Textularia bocki*	*Textularia calva*	*Textularia* sp.	*Trochammina inflata*	*Adelosina bicornis*	*Adelosina laevigata*	*Adelosina mediterranensis*	*Adelosina* sp.	*Comuloculina* sp.	*Comuspira incerta*	*Comuspira involvens*	*Lachlanella undulata*	*Massilina secans*	*Miliolinella subrotunda*	Miliolid undetermined	*Pyrgo inornata*	*Pyrgo* sp.
1	-73																					
2	-93																					
3	-113																					
4	-122																					
5	-133																					
6	-246																					
7	-266																					
8	-286																					
9	-334										*											
10	-354																					
11	-374																					
12	-394																					
13	-414										0.9								0.2			
14	-434										0.5											
15	-484										0.6							1.0	0.4			
16	-496										0.6							0.8				
17	-503										0.2											
18	-524																					
19	-549																					
20	-569										0.8											
21	-589			0.7							1.0											
22	-676										1.2									0.4		
23	-696	0.9									11.6	0.3										0.3
24	-716										1.1											0.4
25	-826										3.6											
26	-766										0.8							0.2	0.2			
27	-786										0.5											
28	-806																					
29	-826										*											
30	-846															*				*	*	
31	-866																					
32	-886							0.4											0.8			
33	-910																					
34	-930																					
35	-950					2.3									0.8	3.1						
36	-970					*																
37	-990																					
38	-1010																					
39	-1030																					
40	-1068																			*		
41	-1088	0.3				0.3					1.7											0.3
42	-1108										6.9						3.0					
43	-1128										*											

44	-1133									5.1		0.6								
45	-1143			0.5						4.7								0.5		
46	-1168																			
47	-1188																			
48	-1218																			
49	-1238																			
50	-1258																			
51	-1278																			
52	-1298																			
53	-1318																			
54	-1338						0.7			4.1										
55	-1368																	0.7		
56	-1388					0.3							0.3							
57	-1408									0.5								1.4		
58	-1428									0.8										
59	-1448																			
60	-1468			0.8														0.3		
61	-1488																			
62	-1529									0.2								0.4		
63	-1549									0.2										
64	-1569									2.9										
65	-1589																			
66	-1609									1.1								0.7		
67	-1629																			
68	-1711																			
69	-1731			0.5						1.4										
70	-1751	0.6		0.6			0.6													
71	-1771					0.7														
72	-1791								0.7											
73	-1818			3.1		0.3	2.8	0.3	0.3	0.7										1.0
74	-1838			4.6		0.6													1.1	
75	-1858										*									
76	-1878																	*	*	
77	-1898																			
78	-1918								*											
79	-1938									0.9					2.8			8.5		
80	-1969			1.9										1.9						
81	-1989																	1.8		
82	-2009																			
83	-2029								*						*					
84	-2049									12.3										
85	-2069		0.9							2.7					0.9					1.8
86	-2089									1.9		1.9			2.8			3.7	2.8	

Quinqueloculina depressa	*Quinqueloculina lata*	*Quinqueloculina longirostra*	*Quinqueloculina oblonga*	*Quinqueloculina seminula*	*Quinqueloculina stelligera*	*Quinqueloculina vulgaris*	*Quinqueloculina* sp.1	*Quinqueloculina* sp.2	*Triloculina dubia*	*Triloculina marioni*	*Triloculina rotunda*	*Acervulina inhaerens*	*Ammonia beccarii*	*Astacolus crepidulus*	*Asterigerinata mamilla*	*Aubignyna perlucida*	*Bolivina difformis*	*Bolivina dilatata*	*Bolivina pseudoplicata*	*Bolivina striatula*	*Bolivinellina pseudopunctata*	*Brizalina spathulata*	*Brizalina variabilis*	*Buccella granulata*
													*											
													*											
													*											
													*											
													*											
				*									*											
													*											
													*			*								
	3.6			9.6	0.2		0.2						46.2			0.2							0.7	
				7.6	0.9		0.7						64.8			0.2					0.2		0.4	
	1.6			11.5	3.2		2.0	0.6					48.3										0.4	
				0.8	1.4		0.2						44.7											
				0.6			1.2						49.8								0.2		0.6	
				2.6									45.2										0.3	
	0.3			0.3									39.8			3.3							1.2	
	3.1												57.3	0.3		0.5							20.7	
				0.3									58.4			1.4	0.3						13.7	
				0.4									46.6			0.4	0.8						12.0	
				0.6	0.9								52.2			0.3	0.9	4.1		0.9	5.7	2.2	11.3	
					1.8		0.4						47.3			2.2	3.6	3.2			14.4	1.1	8.7	
					0.4								27.3				2.8	3.2			20.2	0.8	19.0	
				1.0	0.6		0.2						64.2		0.2	0.6		2.7	0.2		0.4		3.3	0.2
													67.7										1.0	
			0.7	1.3									65.2			0.7		0.2					3.5	0.2
					*								*		*								*	
			*	*									*		*							*	*	
													*										*	
			1.6					0.4					74.9		1.6				0.4		3.7	0.8	0.8	
		0.4	0.9	1.3	1.3								21.9								0.4		0.4	
	0.4			0.8									52.7		1.2								0.4	
0.8			1.6		14.7		12.4						11.6		9.3				3.1			2.3	7.0	
*				*			*						*		*	*			*		*		*	
				*																				
			*	*									*											
			*	*									*											
													*										*	
0.7			1.0	10.7	5.3		1.7				1.7		36.0		7.0	11.0			0.3				1.7	
			11.9	3.0			4.0						45.5			4.0							3.0	
			*	*			*						*		*									

		0.6			3.8							36.7		36.7								1.3			
		0.5	2.3	3.3	4.2			0.9			4.7	23.0		29.6	0.5							0.5	2.8		
1												*													
2					*							*													
3												*													
4																									
5					*							*													
6																									
7												*													
8												*										*			
9					*							*										*			
10					0.7			1.4			0.7	81.6										0.7			
11					0.3							92.4					0.7					0.3			
12					1.1							65.3		0.3								1.1			
13					5.9							58.4										0.5			
14					0.8							85.8					0.8								
15					9.2					0.7		43.9										0.3			
16			0.3	0.3	6.8			0.5			1.5	62.5							0.3			0.3			
17												*													
18			0.4	0.2	1.2			0.2				60.0							1.2			0.4			
19					1.3						1.1	73.2										0.8			
20					7.8							69.6					2.0								
21			0.3		2.8					1.0		90.6													
22					2.9					1.1	0.4	42.1		1.8								1.1			
23					1.9							75.3													
24				1.8	1.1			0.7				40.2		1.8				0.4				0.4			
25					2.8				0.5			49.3		0.5											
26		2.3			3.4							46.6		0.6	0.6				4.5			1.1			
27		0.7								0.7		69.2		0.7								0.7			
28					2.0					0.7		20.7		1.3											
29					2.4			1.7		1.7	1.0	18.3		2.4			0.3	0.3	0.3			3.1			
30				1.7	6.9			1.1	0.6	1.1		9.2			5.2							5.2			
31					*		*	*		*		*			*							*			
32					*					*		*													
33																									
34		*			*							*													
35		2.8		2.8	7.5			7.5				4.7		0.9	7.5		1.9		1.9	5.7	6.6				
36					19.0			2.9				9.5			9.5		5.7			1.9					
37	2.7				25.2			1.8	2.7	0.9		9.0			4.5		0.9		1.8			8.1			
38				*	*			*			*	*		*								*			
39	*	*			*			*				*		*								*			
40					23.4			3.2				20.1										5.2			
41	2.7				5.4			0.9			6.3	7.1	4.5									13.4			
42			5.6	1.9	8.3	1.9		5.6			0.9		22.2				1.9		0.9						
43																									
44																									
45																									
46																									
47																									
48																									
49																									
50																									
51																									
52																									
53																									
54																									
55																									
56																									
57																									
58																									
59																									
60																									

Bulimina aculeata	*Bulimina elongata*	*Bulimina gibba*	*Bulimina marginata*	*Buliminella elegantissima*	*Cassidulina carinata*	*Cassidulina obtusa*	*Cibicides lobulatus*	*Cibicides* sp.	*Cribroelphidium magellanicum*	*Cribroelphidium oceanensis*	*Cribroelphidium poeyanum*	*Cribroelphidium selseyense*	*Cribroelphidium williamsoni*	*Elphidium advenum*	*Elphidium crispum*	*Elphidium earlandi*	*Elphidium flexuosum*	*Elphidium gerthi*	*Elphidium incertum*	*Elphidium macellum*	*Elphidium margaritaceum*	*Elphidium* sp.	*Epistominella vitrea*	*Favulina melo*
												*												
												*												
												*												
												*												
												*												
																						*		
												*										*		
											*	*	*											
				0.2						9.2	1.3	4.0						1.8						
										5.8		2.9						0.2						
				0.2						12.9		3.8						0.2	0.2					
										25.0		4.2	0.2					0.6						
				0.8						24.0		4.9	1.8											
										11.0		0.6												
										48.1	3.0		0.3											
										7.7		2.3	0.5											
										12.7		4.1												
		0.8								13.5	1.2	17.1												
		0.9								0.6	0.6	3.1												
		0.7								0.7	0.7	11.9												
		2.0									1.2	17.8												
										0.2	1.7	8.3						1.5	0.2	0.4				
		0.5										21.0												
										0.2	0.7	18.7												
																							*	
							*																*	
												*												
		1.2									2.1	8.2							0.4					
												72.4												
									0.8		2.1	36.2									0.4	0.4		
				1.6			2.3	2.3				3.1												
									*															*
											*	*												
												*												
												*												
										*	*	*									*			
	0.3	0.3							0.3		2.3	8.0		0.7			0.3	1.0	1.3		1.7			
		2.0										5.9					1.0	1.0				6.9		
										*	*							*						

	0.6									1.9	1.9	3.8						1.3		0.6		
		1.4							1.4	1.4	1.9	5.6			0.5			3.8	1.4	0.9		
										*		*										
																		*				
											*	*										
												*										
												*										
										0.7		8.2						0.7				
										0.3	1.0	2.3										
		0.3									1.7	23.5							1.4			
		0.5								0.5	2.3	20.1						0.9			0.5	
												11.8										
	1.3										5.6	35.1										
											3.3	14.4										
												*										
0.2		3.0					0.2				7.3	19.0							0.6			
	0.2	0.4	0.2		0.2						2.3	16.5					0.2					
												11.8										
	1.0	0.3									0.3	3.5										
	0.7	4.0									2.6	35.9										
											0.6	22.2										
	0.4	2.2									3.0	34.6										
0.5		4.2									7.5	26.3						1.9				
0.6		4.5								0.6	3.4	25.6			1.1							
	0.7	2.1									7.7	11.9			2.1							
2.0		0.7										47.4	0.7					4.7				
	3.4	10.7				1.0				1.0	4.1	24.5			0.3		1.0	0.7		0.3		
	1.1	5.7				0.6	0.6				6.3	28.2			1.7			1.7	0.6			
												*							*			
											*	*							*			
												*										
											*								*			
							0.9															
	1.0	3.8									2.9	12.4							2.9			
		8.1									21.6	3.6							3.6			0.9
												*										
		*									*	*										
		3.9									22.1	7.8							0.6			
		3.6					3.6					25.0							0.9			
										3.7		14.8						0.9				

Fissurina lucida	*Fissurina marginata*	*Fissurina* sp.	*Fursenkoina schreibersiana*	*Gavelinopsis praegeri*	*Globobulimina* sp.	*Haynesina depressula*	*Haynesina germanica*	*Lagena semistriata*	*Lagena sulcata*	*Lagena vulgaris*	*Nonionella opima*	*Nonionoides turgida*	*Patellina corrugata*	*Rectuvigerina compressa*	*Reussella aculeata*	*Reussoolina laevis*	*Rosalina anomala*	*Rosalina globularis*	*Rosalina irregularis*	*Rosalina valvulata*	*Rosalina williamsoni*	*Rosalina* sp.1	*Rosalina* sp.2	*Spirillina vivipara*
							*																	
							*																	
							*																	
							*																	
							*																	
							*																	
							*																	
							*																	
							21.7																	
							15.8																	
						0.2	12.5																	
							21.6																	
							15.9																	
						0.3	40.0																	
							3.9																	
							6.9																	
							6.9																	
							5.6																	
0.3							1.6																	
1.4							0.4																	
0.4							1.2																	
4.4				0.4		0.4	6.7													0.2				
							9.2																	
1.5							7.0																	
							*																	
							*		*															
	0.8		0.4			0.4		0.4																
						0.4	0.4																	
							4.1																	
				0.8			7.8													7.0				
*				*			*												*					
							*														*			
		0.3					3.0													0.7				
							2.0																	

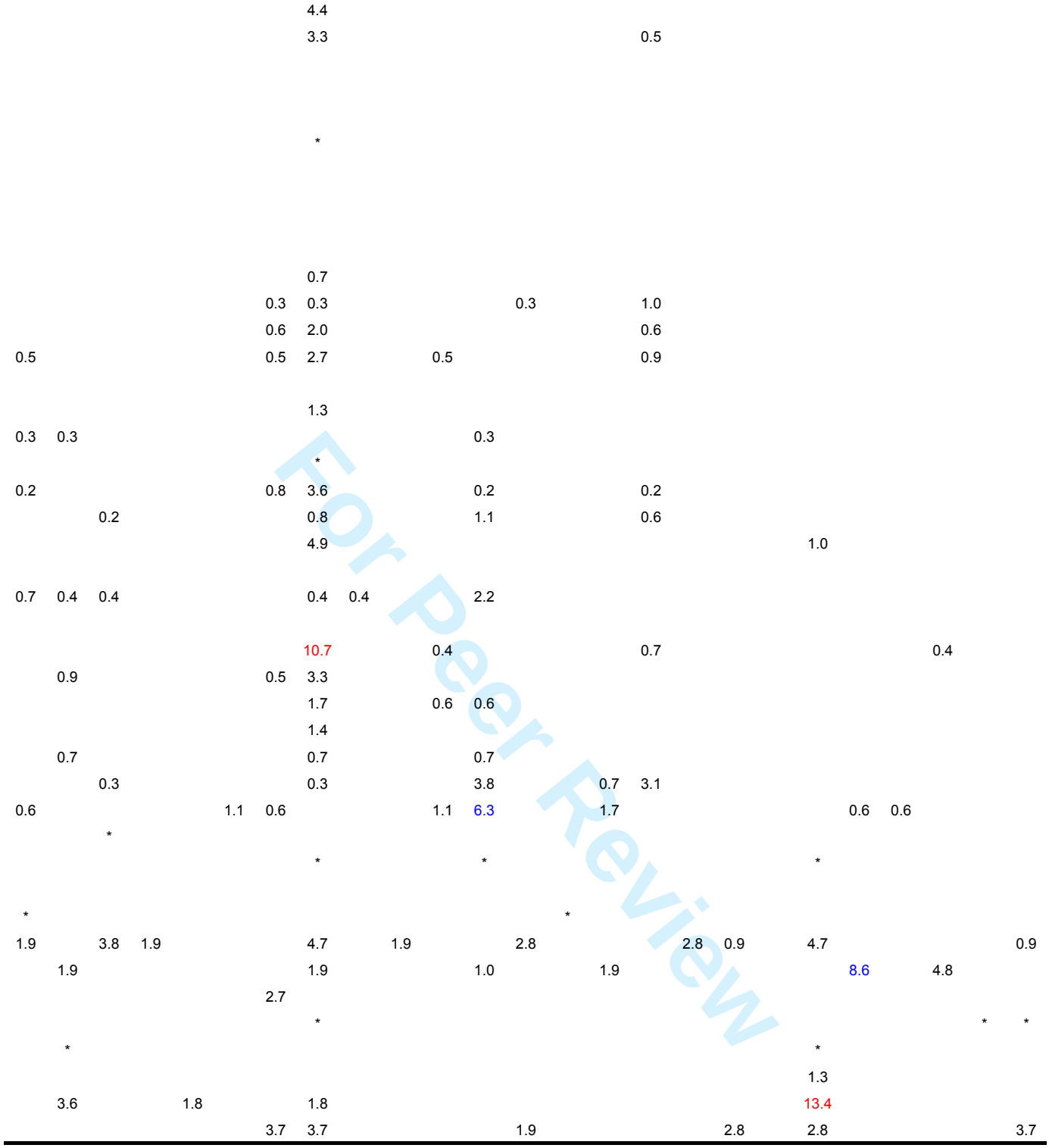

Svratkina sp.	*Tretomphaloides concinnus*	*Trifarina angulosa*	*Uvigerina peregrina*	*Valvulineria bradyana*	Number of foraminifera studied	Number of species	Fisher alpha index	Agglutinated tests %	Porcellaneous tests %	Hyaline tests %	Marine tests %
					3	3	-	-	-	-	-
					0	0	-	-	-	-	-
					3	3	-	-	-	-	-
					3	3	-	-	-	-	-
					3	2	-	-	-	-	-
					3	2	-	-	-	-	-
					7	2	-	-	-	-	-
					6	2	-	-	-	-	-
					23	7	-	-	-	-	-
					2	1	-	-	-	-	-
					1	1	-	-	-	-	-
					29	6	-	-	-	-	-
					448	16	3.24	0.0	14.7	85.3	7.8
					551	12	2.39	0.0	9.8	90.2	2.9
					497	17	3.92	0.0	20.9	78.7	11.0
					501	11	2.21	0.0	3.8	96.2	3.5
					508	11	2.20	0.0	2.0	98.0	3.0
					345	7	1.24	0.0	2.6	97.4	0.6
					337	9	1.70	0.0	0.6	99.4	1.5
					391	10	2.10	0.0	3.9	96.1	24.9
		0.3			291	11	2.26	0.7	1.3	98.0	15.3
					251	12	2.63	0.0	2.0	98.0	15.2
				0.3	318	21	5.05	0.9	13.7	85.4	41.0
					277	17	4.31	0.0	3.7	96.3	36.8
0.4					253	14	3.47	0.0	4.0	96.0	52.5
0.2	0.2			0.2	481	28	6.83	0.0	3.0	97.0	17.1
					195	6	1.42	0.0	0.5	99.5	2.0
					454	12	2.50	0.0	2.0	98.0	6.4
					28	7	-	-	-	-	-
	*				55	14	-	-	-	-	-
					12	3	-	-	-	-	-
	0.4				243	19	4.82	0.4	2.8	96.8	14.4
					228	10	2.14	0.0	3.9	96.1	3.8
	0.4				243	12	2.94	0.0	1.2	98.8	4.0
	6.2				129	20	7.12	2.3	32.6	65.1	71.3
	*			*	84	18	-	-	-	-	-
					18	3	-	-	-	-	-
					15	4	-	-	-	-	-
					12	4	-	-	-	-	-
*					33	11	-	-	-	-	-
					300	28	7.92	0.6	23.1	76.3	28.7
					101	14	4.41	0.0	28.8	71.2	39.6
					29	9	-	-	-	-	-

		0.6				158	15	4.07	0.0	10.1	89.9	47.5
						213	25	7.77	0.5	21.1	78.4	60.1
						9	3	-	-	-	-	-
						4	3	-	-	-	-	-
						36	3	-	-	-	-	-
						8	3	-	-	-	-	-
						0	0	-	-	-	-	-
						29	1	-	-	-	-	-
						43	3	-	-	-	-	-
						41	4	-	-	-	-	-
						147	11	2.75	0.7	6.9	92.4	8.3
						301	12	2.50	0.0	1.0	99.0	1.6
					1.7	357	14	3.17	0.3	1.1	98.6	6.9
					3.7	219	17	4.65	0.0	7.8	92.2	9.9
						127	5	1.31	0.0	1.6	98.4	0.8
	0.3				2.3	305	10	2.23	0.0	9.9	90.1	4.9
					8.1	395	16	3.61	0.8	9.7	89.5	13.3
						11	3	-	-	-	-	-
	0.2				0.2	495	22	5.27	0.0	2.6	97.4	8.8
	0.2				0.2	471	18	3.97	0.0	2.6	97.4	5.6
						102	7	1.70	0.0	10.7	89.3	3.9
						287	8	1.53	0.0	4.1	95.9	2.6
	1.1					273	19	4.97	0.0	6.2	93.8	12.5
						162	4	0.98	0.0	1.9	98.1	0.0
					1.1	271	16	4.02	0.0	3.6	96.4	10.3
						213	14	3.68	0.5	4.7	94.8	10.9
		0.6				176	20	5.81	1.8	5.7	92.5	17.7
					1.4	143	13	3.84	0.7	1.4	97.9	9.8
					17.3	150	14	4.15	0.0	3.4	96.6	26.8
			0.7	0.3	3.1	290	35	10.83	6.5	8.8	84.7	48.1
					3.4	174	29	9.94	5.2	12.5	82.3	44.0
						32	11	-	-	-	-	-
						38	11	-	-	-	-	-
						2	1	-	-	-	-	-
		*			*	42	12	-	-	-	-	-
	7.5	1.9		0.9		106	28	12.42	0.0	32.8	67.2	69.5
					4.8	105	20	7.33	1.9	21.9	76.2	39.3
						111	17	5.60	0.0	35.1	64.9	34.1
						31	11	-	-	-	-	-
						85	14	-	-	-	-	-
						154	10	2.39	0.0	38.9	61.1	26.5
						112	19	7.09	0.9	20.7	78.4	58.3
						108	23	8.95	0.0	37.3	62.7	40.1
						14247	**101**					